Alchemical hydration free-energy calculations using molecular dynamics with explicit polarization and induced polarity decoupling: an On–the–Fly polarization approach

Braden D. Kelly*,† and William R. Smith*,†,‡,¶

†*Department of Mathematics and Statistics, University of Guelph, Guelph ON N1G 2W1, Canada*

‡*Department of Chemical Engineering, University of Waterloo, Waterloo ON N2L 3G1, Canada*

¶*Faculty of Science, Ontario Tech University, Oshawa ON L1H 7K4, Canada*

E-mail: bkelly08@uoguelph.ca; bilsmith@uoguelph.ca

Keywords: molecular simulation, alchemical free energy, molecular dynamics, polarization, solvation, hydration, druglike molecules

January 6, 2020

Abstract

We present a methodology using fixed charge force–fields for alchemical solvation free energy calculations which accounts for the change in polarity that the solute experiences as it transfers from the gas-phase to the condensed phase. We update partial charges using QM/MM snapshots, decoupling the electric field appropriately when updating the partial charges. We also show how to account for the cost of self-polarization. We test our methodology on 30 molecules ranging from small polar to large drug–like molecules. We use Minimum Basis Iterative Stockholder (MBIS), Restrained Electrostatic Potential (RESP) and AM1-BCC partial charge methodologies. Using our method with MP2/cc-pVTZ and MBIS partial charges yields an Average Absolute Deviation (AAD) of 6.3 kJ·mol^{-1} in comparison with the AM1–BCC result of 8.6 kJ·mol^{-1}. AM1–BCC is within experimental uncertainty on 10% of the data compared to 30% with our method. We conjecture that results can be further improved by using Lennard–Jones and torsional parameters refitted to MBIS and RESP partial charge methods that use high levels of theory.

1 Introduction

Molecular simulation using classical force–field (FF) methodology is increasingly being used to calculate thermodynamic properties. One of the most significant is the chemical potential, which is important for applications such as calculations of chemical reaction equilibria,[1–3] phase equilibria,[4,5] solubility,[6–8] hydration free energies ($\Delta G_{\rm hyd}$),[9–12] and protein binding.[13–19] The accuracy of the simulations is dependent both on the quality of the FF, which requires parameters for intramolecular bonds, intermolecular van der Waals and electrostatic interactions, and on the accuracy of the simulation algorithm used.

A common feature of classical FF algorithms, primarily for reasons of computational efficiency, is the use of point charges of fixed magnitudes placed at fixed atomic centers to model the electrostatic interactions. The partial charges are typically calculated in the vacuum state prior to the simulation, without the influence of the ensuing solution environment, using the HF/6-31G* level of electronic structure (ES) theory or using *ad–hoc* corrections meant to make a simpler charge method equivalent to HF/6-31G*. Partial charges calculated at this level in vacuum implicitly include polarization effects not present in vacuum, but are intended to mimic polarization effects present when the solute is in a condensed phase,[20] but are not specific to any particular solvent. Zhou *et al.* recently bench–marked several Electronic ES methods and found that HF/6-31G* varied from under–polarizing on one extreme to over–polarizing by 35% in gas phase calculations on the other.[21]

In a typical molecular dynamics (MD) alchemical $\Delta G_{\rm hyd}$ calculation, the solute molecule's Coulombic interactions with the solvent are first decoupled through a sequence of steps (windows), followed by decoupling of its Lennard–Jones (LJ) interactions. The former is by far the largest contribution, and in a fixed–charge simulation the solute's partial charges maintain constant magnitudes as they are simultaneously decoupled from the solvent. The lack of polarization inherent in the use of fixed–charge FF's is a well–known problem[22] that affects many properties, and several methods to incorporate its effects have been developed. The commonest approaches are to develop explicitly polarizable FFs that allow either the

magnitudes[23–28] or the positions[29,30] of the solutes partial charges to fluctuate, or alternatively to add additional FF terms such as atomic dipoles.[31]

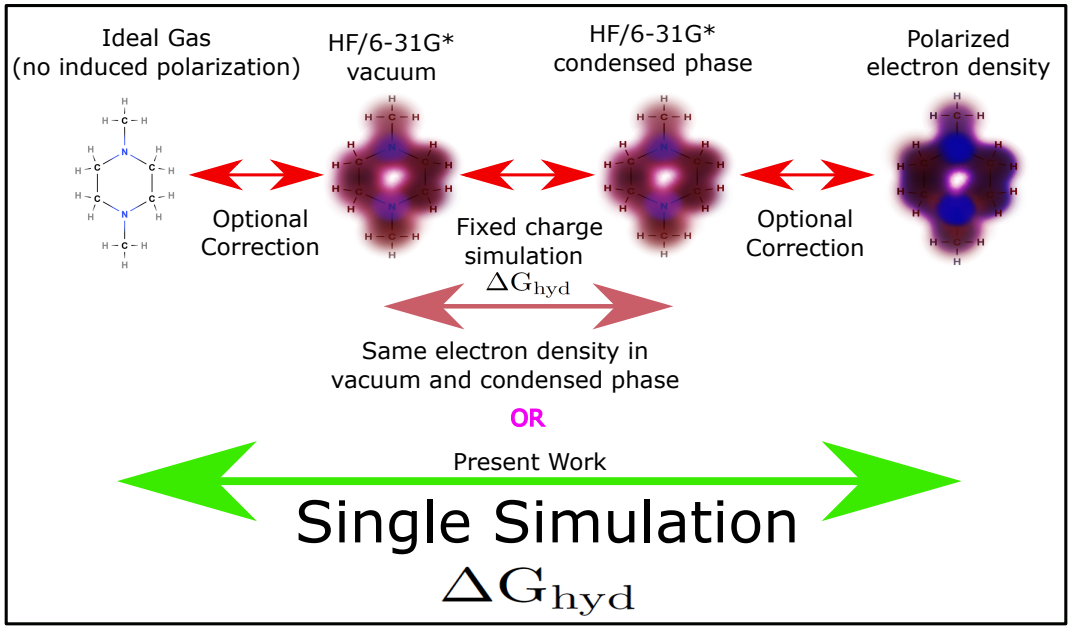

Figure 1: Hydration free energy as the difference between an ideal gas and polarized solute molecule

One approach is to implement post–processing after the fixed-charge MD calculation. This involves the use of ES software, and incorporates the solvent's effect on the solute molecule either implicitly or explicitly. The simplest method is to account for these effects using a self–consistent reaction field (SCRF) within the ES software. Swope *et al.*[32,33] and Riquelme *et al.*[34] recently used this approach, by calculating the free energy required to polarize the solute molecule. Swope *et al.* used PCM (Polarized Continuum Model) calculations and Riquelme *et al.* used SMD (Solvation Models based on Density) calculations to correct MD alchemical free energies for the cost of polarizing the solute molecule. These methods are computationally efficient, since they require only the post–processing of a classical MD simulation and use implicit solvent for the polarization correction.

An alternative to using an SCRF calculation (implicit solvent) to correct for polarization is to correct the endpoints of the free energy calculation using Quantum Mechanical Molecular Mechanics (QM/MM); this approach is termed the *reference potential method*.[35,36] In this case,

the endpoints of the simulation are corrected as per the top portion of Figure (1) by treating the solute at the QM level and the surrounding solvent at the MM level. The endpoints are perturbed to extend the path from beginning to end to match that of an un–polarized solute in vacuum and a polarized solute in solution. Other methods have been developed which also use QM/MM calculations to calibrate the intramolecular FF parameters while also correcting the reference potential.[36] In either case, the endpoint trajectories are re–sampled at intervals and the potential energy is calculated using both a QM/MM calculation and a strictly MM calculation. The difference in potential energy is used in a free energy perturbation scheme to polarize the solute at the QM/MM level. This has the inherent advantage common to all post–processing schemes, in that the QM/MM calculations can be run in parallel, and in theory can be done quickly while the bulk of the calculations are done in the classical fixed charge MD simulation. Convergence requires sufficient sampling, and there are indications that the perturbation between the MM and QM/MM results must be reasonably small.[37–40] It is also often the case that this use of QM/MM makes the estimated free energy of hydration worse than using the MM approach alone.[41] The method has recently been applied to hydration free energy simulations of organic molecules and, in conjunction with the IPolQ-Mod partial charge method, yielded results similar to standard RESP and AM1–BCC free energies with GAFF on small test sets.[35,42]

IPolQ is a recently developed method that calculates the electron density distribution of the solute based on measurements taken during explicit water simulation,[43] and then employs it to calculate polarized restrained electrostatic potential (RESP).[44] These charges are then averaged with charges derived for the solute in vacuum. This method is the default atomic charge method for the AMBER ff14ipq[45] and ff15ipq[46] FFs. The advantage of this approach is that polarity is explicitly involved in the charge calculations, and with much higher levels of QM theory (MP2/cc-pV(T+d)Z) rather than relying on the over–polarization exhibited by using HF/6-31G* in vacuum simulations to mimic liquid phase effects.[21,47] While providing more consistent partial charges, IPolQ still suffers from having incorrect polarization in each

endpoint when used in free energy calculations, since both endpoints are half polarized to the same degree.

The IPolQ-Mod method has been developed recently as a simpler form of the IPolQ method by using implicit solvent to polarize the solute partial charges by Muddana *et al.*[47] where they found it closely matched solvation free energies calculated using RESP partial charges derived from HF/6-31G* vacuum calculations. A comprehensive comparison has also been made between using default RESP partial charges and IPolQ-Mod charges by Mecklenfeld and Raabe.[48]They found that both methods give similar results. This approach has also been used recently for free energy calculations by Jia and Li[35] and by Jia[35] and a modified form was used by Riquelme *et al.*[34] Jia and Li found slightly improved results over those of the classical RESP partial charges on a small test set of molecules when using IPolQ-Mod. When correcting the endpoints using QM/MM, Jia and Li[35] and Jia[42] found the results improved and were similar to AM1–BCC. Riquelme et al's IPolQ-Mod results when using Minimal Basis Iterative Stockholder (MBIS)[49] charges rather than RESP charges achieved lackluster results in comparison with the simple and general AMBER force field (GAFF)[50] default charge method AM1–BCC,[51] and with their proposed method that used MBIS charges with post–simulation implicit polarization corrections.

All methods mentioned thus far that attempt to account for polarization effects without the use of additional parameters (with the exception of SMD,[52] which is parameterized to fit experimental hydration free energy data), either pre– or post–simulation, treat the interaction in a fixed averaged way rather than dynamically, and thereby suffer a similar flaw: the dynamics of the actual MD simulations is implemented using fixed charges and is unaccountably affected by this simplification. The previously mentioned methods account for solute self-polarization costs to varying degrees, but do not account for the polarization cost of rearranging the solvent as the solute interacts and becomes polarized by the changing environments.

A more computationally expensive method has also been used by Reddy *et al.* for relative

free energy calculations that encapsulates the dynamics of the simulation, termed QM/MM-FEP (quantum–mechanical–based free energy perturbation[53–55]). At every MD step the energy and its gradients in the QM zone are calculated using semi–empirical AM1, while the QM/MM and MM interactions are calculated using the MM FF. QM/MM solvation free energies using a potential of mean force (PMF) approach that updates the mean charge distributions for the solvent has also been used by Rosta *et al.*[56] Similar to the approach of Reddy *et al.* , all interactions between the QM and MM region are calculated using a MM FF, although partial atomic charges for the solute are calculated using implicit solvent (Polarizable Continuum Model, PCM).

Importantly, for the test set of organic molecules in the present study, Reddy *et al.* applied their method to alkylamines and successfully predicted the signs of the hydration free energies, whereas the corresponding pure MM FF failed.[54] In the QM/MM-FEP method, alchemical windows are calculated in serial order, and partial charges on the solute are updated at the initiation of each window's simulation using HF/6-31G** electrostatic potential (ESP) derived charges. Whereas significant improvements were shown over the corresponding MM FF results, there is a nontrivial computational cost in using QM at every MD step, and to compensate, a low semi–empirical QM level was used. This method has the advantage that intramolecular parameters are not required, and as increased computational speeds become available, higher QM levels can be used for both the QM region's energy and gradient calculations, and more sophisticated methods can be used to obtain the partial charges, for instance MBIS and RESP rather than ESP.

An intuitively attractive way to allow the partial charges of a solute molecule to dynamically evolve during a simulation is to update the charges in the course of the simulation. This approach has been carried out by Maranon et al.[57,58] to study structure and hydrogen bonding in biomolecular simulations, where charge updates were dynamically implemented based on the solute's geometry in an implicit solvent. A more rigorous method that polarizes the solute in the presence of explicit solvent was developed by Kimura *et al.* .,[59] who updated

the partial charges of the solute using QM/MM snapshots during the free energy calculations. They employed multiconfigurational RESP charges calculated at the HF/6-31G** level. They found that this method overpolarized the solute and the resulting free energies showed large errors in comparison with experiment. They overcame this problem by empirically scaling the RESP charges by an ad–hoc factor of 0.9.

The goal of this paper is to propose and test a new method (on–the–fly–polarization: OTFP) for more accurately capturing the contribution of the electrostatic interactions in a hydration free energy simulation than has been achieved by previous approaches. We present results at 298.15 K and a pressure of 1 bar for a test set of 30 molecules containing C/H/N/O atoms, of various structures and sizes. We show results calculated using both fixed–charge FF methods, and our OTFP method. We show results using several charge derivation methods: MBIS at both the B3LYP/cc-pVTZ and MP2/cc-pVTZ levels, RESP at both HF/6-31G* and B3LYP/cc-pVTZ, in addition to AM1-BCC. We compare our results with those in the FreeSolv[12] database, in addition to those calculated by Riquelme et al.[34] using their MBIS method with post–simulation SMD polarization corrections.

The paper is organized as follows. In the next section, we summarize the simulation methodology, including the FF generation methods and our OTFP on–the–fly methodology for periodically updating the partial charges with the explicit water solvent and electric field decoupling. We then describe the test set and the simulation protocols used. This is followed by a section describing the results and their discussion, followed by our conclusions and recommendations.

2 Simulation Methodology

The *intrinsic* hydration free energy (hereafter we drop the adjective) is the molar free energy change when a single solute molecule is inserted into pure water solvent when both phases

are at the same density.

$$\Delta G_{\rm hyd}(T,P) = \mu^{{\rm res},NVT;\infty}_{\rm solute}[T,\rho_{\rm solv}(P,T)] \tag{1}$$

where $\rho_{\rm solv}(P,T)$ is the solvent density at the specified values of T and P and $\mu^{{\rm res},NVT;\infty}_{\rm solute}[T,\rho_{\rm solv}(P,T)]$ is the residual chemical potential of the solute at infinite dilution in the solvent. Hydration free energies may be obtained experimentally by measuring the aqueous solubility of the solute in solution at a particular temperature, and its partial pressure in the vapour phase in equilibrium with the solution, at a sufficiently low concentration that the solute chemical potential can be expressed in Henry-Law form with the density concentration variable and the pressure is sufficiently low that ideal gas behaviour in the vapour phase holds. The solute's vapour-liquid equilibrium is governed by the equality of its vapour and solution phase chemical potentials:

$$\begin{aligned}\mu^0_{\rm solute}(T;P^0) + RT\ln\left(\frac{P^{\rm vap}_{\rm solute}}{P^0}\right) &= \mu^0_{\rm solute}(T;P^0) + RT\ln\left(\frac{xRT\rho^*_{\rm solv}(T,P)}{P^0}\right) \\ &\quad + \mu^{{\rm res},NVT;\infty}_{\rm solute}[T,\rho_{\rm solv}(T,P)]\end{aligned} \tag{2}$$

$\mu^0_{\rm solute}(T;P^0)$ is the ideal–gas chemical potential of the pure solute at T and the reference state pressure P^0, $P^{\rm vap}_{\rm solute}$ is its partial pressure in the vapour phase, $\rho_{\rm solute}(T,P;x)$ is the solute density at the specified T,P and mole fraction x, and $\mu^{{\rm res},NVT}_{\rm solute}[T,\rho_{\rm soln}(T,P;x)]$ is the solute residual chemical potential at the solution (T,P,x). Eqs (1) and (2) yield

$$\frac{\Delta G_{\rm hyd}(T,P)}{RT} = \left(\frac{P^{\rm vap}_{\rm solute}}{xRT\rho^*_{\rm solv}(T,P)}\right) \tag{3}$$

There may be experimental deviations if the solute concentration or its vapour pressure are not sufficiently low as to respectively obey Henry's law or ideal gas behaviour.

We calculate $\mu^{{\rm res},NVT;\infty}[\rho_{\rm solv}(T,P)]$ by incorporating a quantum mechanical strategy to

account for the polarization of the solute in conjunction with the usual free energy change procedure of a standard molecular simulation package such as GROMACS.[60] Similar to the general approach employed by Maranon et al.[57,58] and of Kimura *et al.*,[59] we allow the partial charges of a solute molecule to dynamically evolve by updating the charges during the simulation. Our approach differs in three ways: (1) we use a higher level of ES calculation to avoid implicit polarization in gas–phase ES calculations due to low level theory and/or small basis set; (2) we compare several charge assignment procedures, whereas they used only the multi–configuration RESP method; and (3) we develop an approach for calculating the effect of the solvent electric field so that in a single simulation we sample the free energy difference between an unpolarized solute in vacuum and a polarized solute in solution.

The improved algorithm for calculating ΔG^{hyd} of the solute involves modifications to standard procedures. First, we explore different methodologies for charge assignment in the construction of the FF in vacuum. Second, we introduce a novel approach for calculating the effects of the solute polarization on ΔG^{hyd}. We describe these aspects in the following two sections.

2.1 Force-Field Parameterization

The FFs were generated in four steps: 1) the ES software Spartan'18[61] was used to find all conformers for each molecule using the MMFF94 level of theory. Next, we calculated the equilibrium geometries at the semi-empirical PM6 level of theory. The 20 lowest energy geometries were then recalculated at the HF/6-31G* level of theory; 2) the lowest energy conformer was further optimized at the MP2/aug-cc-pVTZ level of theory if there were fewer than 7 heavy atoms (CNO) or else at the ωB97XD/aug-cc-pVTZ level for the larger molecules; 3) the AmberMD toolpackage Antechamber[62] was used to generate GAFF(2.11) FFs, and when necessary, RESP or AM1–BCC charges. In the latter case, the molecule's geometry was re–optimized at the AM1 level of theory, which is the default and recommended setting in Antechamber. This default setting was over–ridden when solute charges were optimized

periodically during OTFP simulations. HORTON 2.0.0[63] was used for generating minimum basis iterative Stockholder (MBIS) charges. Gaussian16[64] was used for all ES structure calculations of the solute electron density except for AM1–BCC charges, which used the Antechamber sqm software; 4) the python program ACPYPE[65] was used to convert the generated Amber topology for the FFs to GROMACS topology files. An ultra–fine grid was used in HORTON for the MBIS charges.

Many different QM theories exist for electronic structure calculations. We selected B3LYP because it is a common hybrid density functional theory that strikes a balance between computational speed and accuracy. We selected MP2 strictly for its accuracy; it is computationally expensive.

The choice of basis sets was more involved, because we desired accuracy at an affordable cost but we also wanted to avoid potential issues when updating the solute molecule's partial charges via QM/MM snapshot calculations pertaining to charge migration to the QM/MM boundaries.[66] To avoid this, we purposely did not add diffuse functions (aug) to the basis set. A benchmark review was done for dipole moments and polarizabilites relatively recently,[67] and based on its results we chose to use cc–pVTZ as our basis set of choice. In order to compare with standard GAFF protocols we also used HF/6-31G* with RESP, as well as AM1-BCC. This also created reasonable benchmarks for comparisons, since we used GAFF(2) rather than the original GAFF.

For both RESP and AM1–BCC, the fixed charges for equivalent atom types were calculated by averaging via Antechamber's built–in use of OpenEye software.[68] Since this is not available in the HORTON program for MBIS charges, we used a python script to duplicate the averaging procedure used by Antechamber.

2.2 The On–the–fly–Polarization Charge Updating Procedure

In a conventional fixed–charge alchemical free energy change calculation, a solute molecule's electrostatic interaction with its environment is linearly decoupled over a series of λ windows

from $\lambda = 1$ when the solute molecule is fully interacting with the solvent to $\lambda = 0$ when it is fully noninteracting. Linear scaling of the λ parameter is the mathematical equivalent of scaling the solute molecule's partial charges, which achieves the desired decoupling effect of the forces and energies between the solute and solvent (but retains solvent-solvent and all intramolecular interactions). At intervals in the MD simulation we calculate polarized partial charges on–the–fly by taking snapshots of the MD simulation and including the solvent partial charges in the background call to Gaussian when we update the solute's partial charges. We scale the solvent background partial charges by the λ parameter in order for the electric field generated by the solvent, which polarized the solutes electron density, to reflect the decoupled interactions of the solute and solvent. We effectively scale the partial charges of the solvent in the QM/MM snapshot to decouple the electric field produced by the point charge background, and scale the partial charges in the MD simulation to decouple the forces and energies. In this way when the solute is fully coupled to the solvent in the MD simulation the solute partial charges will be fully polarized by the surrounding solvent, and when the solute is fully decoupled from the solvent in the MD simulation the solutes partial charges will be calculated with no influence from the solvent since the solvent partial charges will have been scaled to zero in the QM/MM snapshots. This procedure is illustrated in Fig. (2).

As an example of the difference between a conventional alchemical free energy calculation and our method, we compare the equations used to calculate the free energy perturbation according to a simple forward Zwanzig perturbation expression. For a linearly scaled Coulombic free energy contribution, this is

$$\Delta A_{\mathrm{fwd}} = -RT \ln \left[\sum_{k=1}^{N_k} \left\langle \exp\{-\beta[\mathcal{U}(\lambda_{k+1}|\boldsymbol{q}^0) - \mathcal{U}(\lambda_k|\boldsymbol{q}^0)]\} \right\rangle_k \right] \tag{4}$$

where A is the Helmholtz free energy, N_k is the number of Coulomb windows, $\mathcal{U}_{\mathrm{k}}$ is the potential energy, and $< x >_k$ denotes the ensemble average of the quantity x in window k.

In our method, the partial charges of the solute change both with time in a given window,

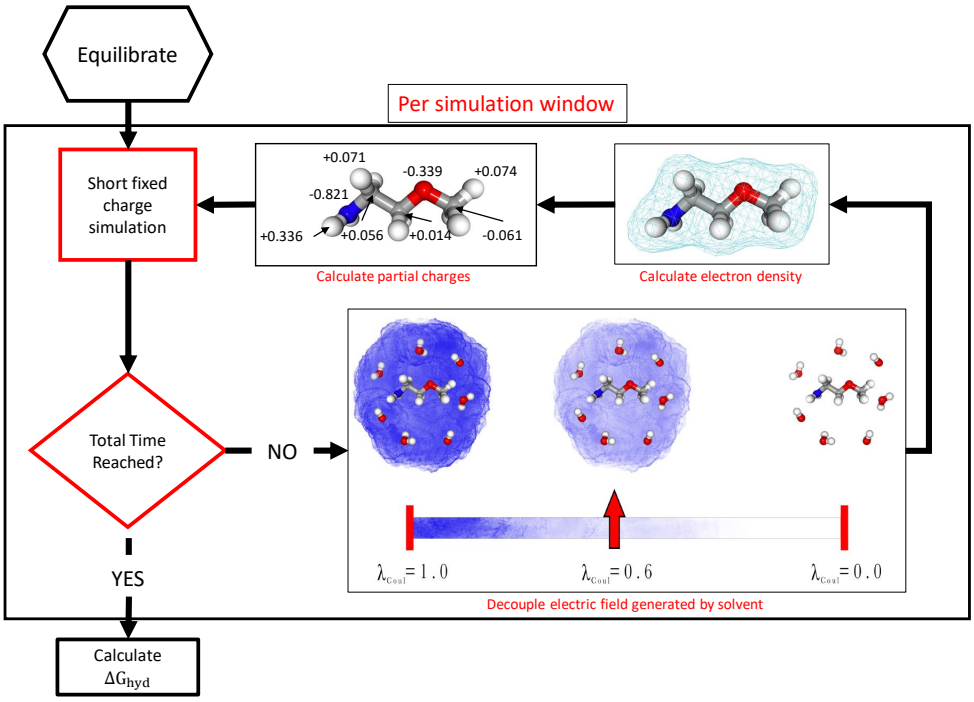

Figure 2: Workflow of partial charge updates with electric field decoupling. First all solvent partial charges within 12 Åof the solute are found and used as a point charge background to explicitly polarize the solute in the QM electron density calculation. The solvent's MM charges are scaled by the coulomb λ, this decouples the electric field generated by the solvent MM partial charges which induces polarization in the solute molecule. The electron density is calculated, and then partitioned into partial charges according to the desired method. Finally, the simulation is continued with the updated charges.

but also in average magnitude in a coulomb window *i.e.*, the average set of partial charges on the solute is different in each Coulomb window. Our free energy is calculated according to

$$\Delta A_{\text{fwd}} = -RT \ln \left[\sum_{k=1}^{N_k} \left\langle \frac{1}{N_j} \sum_{j=1}^{N_j} \left\langle \exp\{-\beta[\mathcal{U}(\lambda_{k+1}|\boldsymbol{q}_j^k) - \mathcal{U}(\lambda_k|\boldsymbol{q}_j^k)]\} \right\rangle_j \right\rangle_k \right] \tag{5}$$

where $\boldsymbol{q}_j^k$ denotes the sample set j of the partial charges on the solute molecule calculated with the explicit solvent electric field strength of window k, N_j is the number of sample sets.

2.2.1 Cost of self-polarization

It is well established that according to linear response theory the cost of polarizing a molecule is half the value of the solute–solvent interaction energy.[69,70] IPolQ methods account for this

cost by using half-polarized partial charges, as discussed earlier. Eqn. (5) sums the differences in potential energy with respect to adjacent windows where both states in the perturbation use the partial charges of the reference window and whose intermolecular coulombic potential energy $\mathcal{U}_{\text{inter}}^{\text{coul}}$ differs by the λ factor. In our case the adjacent windows have charges of different average magnitudes due to polarity differences. The self–polarization cost can be accounted for by using half–polarized partial charges, as is done by IPolQ and IPolQ-Mod. However, this does not account for the costs associated with reorganizing the solvent around the solute due to the latter's differing polarization at each endpoint. We instead take advantage of the fact that we evaluate the free energy difference between state points using MBAR, which uses forward and reverse perturbation sampling. If we denote the two states as a and b then in the forward perturbation we use the partial charge set $\mathbf{q^a}$ on the solute, whereas in the reverse perturbation we use the partial charge set $\mathbf{q^b}$. This results in two sets of potential energy differences being sampled between the two states, $\Delta\mathcal{U}_{a\to b}(\mathbf{q^a})$ and $\Delta\mathcal{U}_{b\to a}(\mathbf{q^b})$. It is straightforward to show that the average of these two potential energy differences is equivalent to using half–polarized charges, *i.e.*,

$$\Delta\mathcal{U}_{ab}(\mathbf{q^a} + \frac{\mathbf{\Delta q}}{\mathbf{2}}) = \frac{\mathbf{\Delta\mathcal{U}_{a\to b}(q^a)} + \mathbf{\Delta\mathcal{U}_{b\to a}(q^b)}}{\mathbf{2}} \tag{6}$$

where $\Delta\mathbf{q} = \mathbf{q^b} - \mathbf{q^a}$ and $\Delta\mathcal{U}_{ab}(\mathbf{q^a} + \frac{\mathbf{\Delta q}}{\mathbf{2}})$ implicitly accounts for the cost of self–polarization. It is not, however, the case that the difference in free energy accounts for the free energy cost of self-polarization, since it involves the exponential (Boltzmann factors) of energy differences. In the case of suitably small arguments in the exponential functions the average of two exponentials with different arguments is approximately equal to the exponential of the average of their arguments.

$$\Delta\mathcal{A}_{\text{ab}}\left(\Delta\mathcal{U}_{ab}(\mathbf{q^a} + \frac{\mathbf{\Delta q}}{\mathbf{2}})\right) \approxeq \frac{\Delta\mathcal{A}_{\text{a}\to\text{b}}(\Delta\mathcal{U}(\mathbf{q^a})) + \mathbf{\Delta}\mathcal{A}_{\text{b}\to\text{a}}(\mathbf{\Delta}\mathcal{U}(\mathbf{q^b}))}{2} \tag{7}$$

where

$$\Delta\mathcal{A}_{\mathrm{a}\to\mathrm{b}} = -RT\ln\langle\exp(-\beta\left[\mathcal{U}(\lambda^b|\boldsymbol{q}^a)-\mathcal{U}(\lambda^a|\boldsymbol{q}^a)\right])\rangle \quad (8)$$

$$\Delta\mathcal{A}_{\mathrm{b}\to\mathrm{a}} = RT\ln\langle\exp(-\beta\left[\mathcal{U}(\lambda^a|\boldsymbol{q}^b)-\mathcal{U}(\lambda^b|\boldsymbol{q}^b)\right])\rangle \quad (9)$$

As validation of the approximation, we compare the Zwanzig and BAR estimators of the Coulomb contributions to the ΔG_{hyd} values for 2-methoxyethanamine and caffeine using both our OTFP sampling and half–polarized potential energies. The results are shown in Tables (S4-S6) of the SI, and indicate that the BAR and Zwanzig estimators using OTFP sampled data provide results equivalent to using half–polarized potential energy samples between each pair of windows. Also shown in Tables (S4-S6) in the SI are comparisons of the MBAR estimator with the Zwanzig and BAR estimators. These show that MBAR is comparable to both Zwanzig and BAR for the Coulomb contributions. Therefore, the use of MBAR with OTFP sampling provides estimators that account for the cost of self–polarization, and in addition accurately handle the LJ contribution.

We also show in Table S3 of the Supporting Information ΔG_{hyd} results for a medium-size polar molecule comparing the standard deviation of 10 independent replicate runs with the MBAR uncertainty estimates of each run. For MBIS partial charges, each MBAR uncertainty estimate (whether for OTFP or fixed charges) provides a slightly conservative estimate of the standard deviation of the replicate runs. This is also the case for RESP partial charges using OTFP, but for fixed charges, each MBAR uncertainty underestimates the replicate run result by about 40%. We take this as validation that the OTFP MBAR uncertainty for a single run is a reasonable surrogate for that arising from independent replicate runs.

Each sample set j consists of a relatively short MD simulation run in window k with solute charges $\boldsymbol{q}_j^k$. These are calculated from the final configuration of the previous run by performing an independent ES calculation that incorporates the partial charges of all solvent molecules within a surrounding shell (we used 12 Å). When updating the solute's partial

charges, we include the solvent's MM partial charges in the background of the electron density calculation, but we scale the value of the solvent's partial charges by the same λ_k used in the corresponding MD window. In this way, the electric field generated by the solvent partial charges is at full strength when the solute is fully coupled to the solvent environment at $\lambda_k = 1.0$ and is fully decoupled at $\lambda_k = 0$.

3 Systems Studied and Simulation Details

We used SPC/E[71] water rather than the typical TIP3P[72] model for simulations using MBIS derived partial charges. This choice of water model was motivated by the findings of Riquelme *et al.*[34] that SPC/E gave a 0.56 kcal·mol^{-1} lower RMSD compared with TIP3P water when using MBIS charges where they tested 613 molecules in the FreeSolv database. We used TIP3P for RESP and AM1–BCC calculations, and we also show results for RESP and AM1–BCC using SPC/E water in the Supporting Information.

We performed hydration free energy calculations for 30 molecules containing C/H/N/O atoms from the FreeSolv database of varying complexity, shown in Fig. (3). We specifically chose to test our method, but not exclusively, on molecules that AM1–BCC struggles with, which we define as having an error over 8.4 kJ·mol^{-1} (2.0 kcal·mol^{-1}). We also included several molecules for which AM1–BCC handles very well, and we also chose some molecules that AM1–BCC both over–estimates and under–estimates the hydration free energy; this is clearly indicated in Fig. (6). This latter point was to ensure that our methodology is not restricted in its usefulness to, for instance, only molecules whose free energies are over-estimated or under-estimated by AM1–BCC.

All simulations were carried out using the GROMACS version 2016.3[73] suite of software for systems with $N = 2000$ water molecules and 1 solute molecule at $T = 298.15$ K and $P = 1$ bar. We first determined the box size, $V(NPT)$ corresponding to the specified N, P, T values, by averaging over 10 independent NPT runs. We initiated each independent NPT

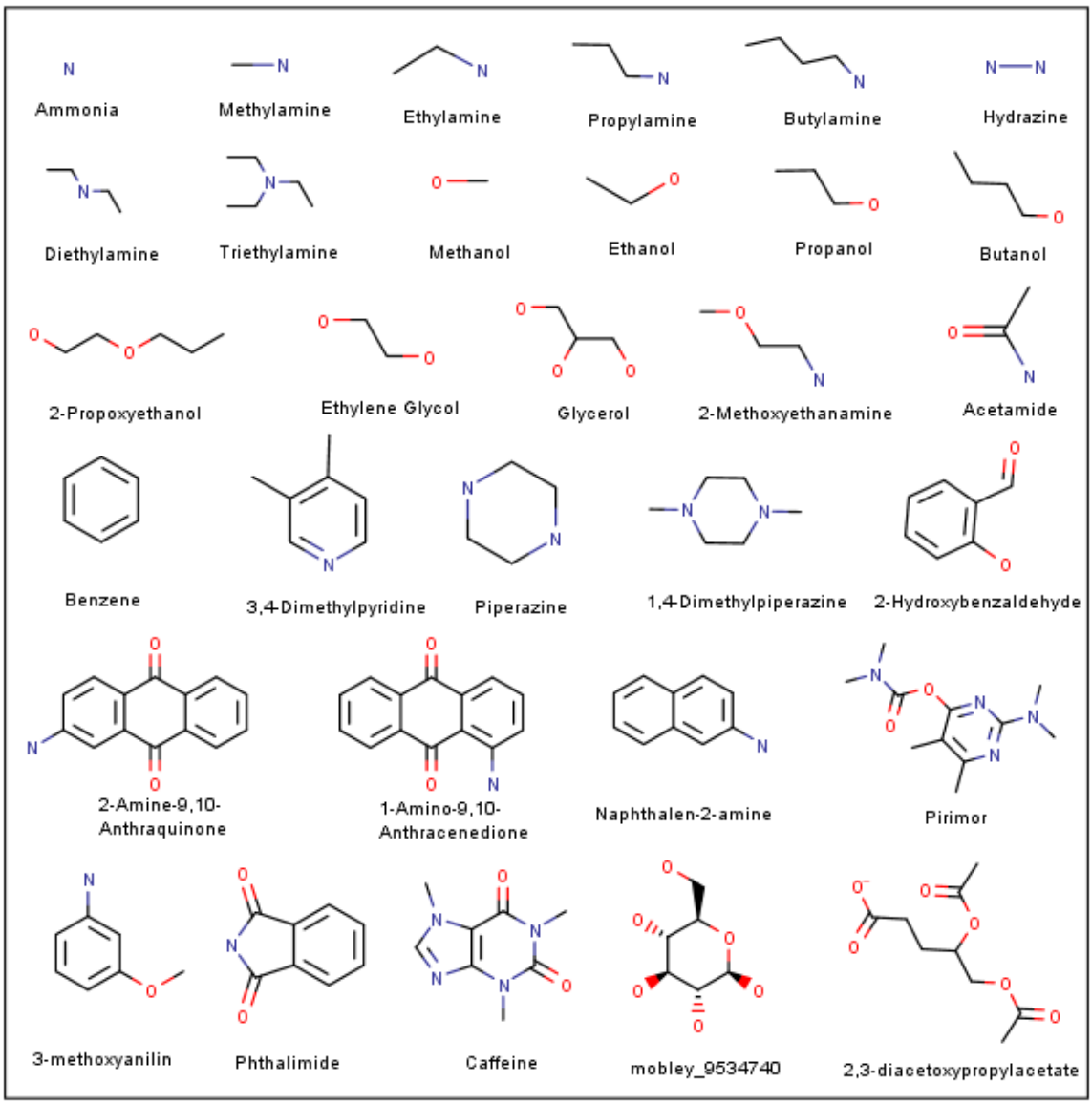

Figure 3: Molecules studied. mobley_9534740 = (2R,3R,4S,5S,6R)-6-(hydroxymethyl)tetrahydropyran-2,3,4,5-tetrol

run by randomly inserting the water molecules into a cubic box of length 4.3 nm using the GROMACS "insert-molecules" function.[74] The steepest descent algorithm was then used to minimize the system energy, terminating after either 20,000 steps or a maximum force of 100 $kJ{\cdot}mol^{-1}nm^{-1}$ was reached. In all cases, the minimization converged to the force constraint before reaching the maximum number of steps. Initial velocities were then assigned according to a Maxwell–Boltzmann distribution at the simulation temperature. An NVT ensemble run

was then equilibrated for 1 ns with a timestep of 2 fs using a stochastic Langevin leapfrog integrator.[75] A Lennard–Jones cutoff distance of 1.2 nm was employed with tail corrections for energy and pressure, and a neighbour list with a cutoff of 1.2 nm was updated every 10 steps. The Particle Mesh Ewald (PME) method was used with real space cutoff of 1.2 nm, tolerance of 10^{-6}, an order of 12 and Fourier spacing of 0.1 nm. We then ran an NPT equilibration run for 5 ns using a Berendsen thermostat with thermo-coupling parameter 0.1 and a Berendsen barostat with pressure-coupling parameter 2.0, compressibility of 4.5×10−5 and reference pressure of 1 bar. Following this we did a production run for 15 ns using a stochastic Langevin leapfrog integrator with a thermo-couple of 1.0 and a Parinello-Rahman barostat with a pressure couple of 5.0, compressibility of 4.5e-5, and reference pressure of 1 bar. The same neighbour list, Ewald criteria and cutoffs were used in all ensembles.

In the ΔG_{hyd} calculations, for every simulation each λ window used unique initial random number seeds to generate positions and velocities in the starting configuration. We carried out energy minimization on each window according to the same criteria as described above for the NPT simulations. Energy minimization was followed by NVT equilibration and production runs, both using the same protocols as the NVT equilibration in the NPT box size simulations. We performed both the conventional fixed–charge simulation and our OTFP simulation starting from the last configuration of the NVT equilibration. We also equilibrated each window with a 2 ns run prior to a 4 ns production run.

Free energy calculations were performed using the Multistate Benedict Acceptance Ratio (MBAR)[76] as implemented in the pymbar/alchemical analysis software.[77] We first decoupled the solute's Coulombic interactions from its solution environment, followed by decoupling of the LJ interactions using λ_{coulomb} = [0.0 0.1 0.2 0.3 0.4 0.5 0.6 0.7 0.8 0.9 1.0] and λ_{LJ} = [0.0 0.05 0.1 0.15 0.2 0.25 0.3 0.35 0.4 0.5 0.6 0.65 0.7 0.75 0.8 0.85 0.9 0.95 1.0]. While it is common to use fewer lambda windows for decoupling the Coulombic interactions, the number 5 being frequently used,[11,12,34] there are important cases where hydration free energies differ markedly when using 5 or 11 windows, notably for Triethylamine, one of the molecules studied

here.[11] To be on the side of caution we always used 10 Coulomb windows. We used a soft–core Lennard-Jones potential with parameters $\lambda = 1$ and $\alpha = 0.5$. Potential energies of all λ windows were sampled every 100 steps for post-processing with MBAR. For each window we updated the partial charges every 20 ps (10,000 steps) with exceptions for four large drug-like molecules (Caffeine, Pirimor,(2R, 3R, 4S, 5S,5R)-6-(hydroxymethyl)tetrahydropyran-2,3,4,5-tetrol, and 2,3-diacetoxypropylacetate) when using MP2/cc-pVTZ, in which case we updated the partial charges every 80 ps.

We explored the effect of system size by solvating 2-Propoxyethanol, a medium–size molecule and Caffeine, a large molecule, in 500, 2000 and 8000 water molecules and measuring the resulting ΔG_{hyd}. We show these results in Table (S2) of the Supporting Information. Since the results for 2000 and 8000 water molecules were equal within their calculated MBAR uncertainties, we used 2000 water molecules for all simulations.

4 Results

In all cases, we calculated ΔG^{hyd} using both a conventional fixed–charge approach and using our proposed OTFP method, each in conjunction with the partial charge and QM theory/basis sets shown in Table 1 as described earlier. Results for each method in comparison with experiment are shown in Figs (4)–(6) as parity plots. The deviations from experiment and statistical measures of agreement of the predicted and experimental results are shown in the figures and summarized in Table 2. The quality of the agreement with experiment of a theoretical approach can be assessed by various empirical and statistical measures. All raw simulation results can be found in the Supporting Information, which enables alternative measures to be calculated. We note in passing that the Pearson R2 statistic is not generally useful for this purpose, due to its well-known deficiencies.[78,79] We refer to our results as either "fixed" or "OTFP". Fixed means the partial charges were calculated in vacuum using the indicated level of theory/basis set, and those partial charges were not updated throughout

Table 1: Partial charge methods and ES details. SPC/E water model results for RESP and AM1–BCC are shown in the Supporting Information.

Present Work				
Charge Method	QM theory	QM basis set	water model	Force–Field
MBIS	B3LYP	cc-pVTZ	SPC/E	GAFF(2.11)
MBIS	MP2	cc-pVTZ	SPC/E	GAFF(2.11)
RESP	B3LYP	cc-pVTZ	TIP3P	GAFF(2.11)
RESP	HF	6-31G*	TIP3P	GAFF(2.11)
AM1–BCC	AM1	-	TIP3P	GAFF(2.11)
Literature Results				
AM1–BCC	AM1	-	TIP3P	GAFF(1.7)[12]
MBIS + SMD	BLYP	def2-TZVP	SPC/E	GAFF(1.7)[34]

the simulation. "OTFP" refers to our method which updates partial charges on the fly and incorporates polarization into the partial charges in each Coulomb window.

4.1 Hydration free energies using MBIS partial charges

Fig. 4 shows parity plots against experimental results using partial charges determined by the MBIS approach, with SPC/E water and different levels of theory (4(a) and 4(b)). Fig. 4(a) shows results obtained by Riquelme *et al.*[34] using a combination of MD and SMD simulations. Fig. 4(b) shows our results using two different levels of theory for the ES calculations; the left figure shows results using B3LYP/cc-pVTZ and the right figure shows results using MP2/cc-pVTZ. We also show results at both levels of theory for fixed charges calculated in vacuum in the Supplemental Information; they serve as baseline indicators for how the results change when using our OTFP method to implement polarization. Both levels of theory used with OTFP produce results aligned more closely to parity with experimental values than the Riquelme *et al.* results. There are fewer outliers and more results are within the experimental uncertainty using OTFP. The best results are obtained using the MP2 level of theory. Both OTFP methods have more than double the number of values lying within experimental uncertainty in comparison with those of Riquelme *et al.*

The Table 2 data shows that the MBIS fixed–charge results for both B3LYP and MP2

Table 2: Comparison of ΔG_{hyd} results for all methods, in addition to existing literature results. All values are in kJ·mol^{-1}. † = cc-pVTZ. χ = def2-TZVP. The Spearman rank correlation coefficient (ρ_s) is a statistical measure between two sets - in this case between simulation and experimental ΔG_{hyd} values, with a value of 1 indicating perfect monotonic rank correlation, 0 indicating no correlation, and -1 indicating perfect negative monotonic rank correlation.[80] AAD is the Absolute Average Deviation (Prediction minus Experiment), AD is the Average Deviation. The Confidence Intervals (CI) for the AD were obtained using the Student–t distribution at the 95% level; the others are 95% CIs obtained by means of empirical bootstrapping using 10^5 resamples with replacement (*e.g.*, Chernick[81]).

Charge Method	Theory/ Basis	Mode	H_2O Model	RMSD	AAD	AD	ρ_s[80]
MBIS	B3LYP/†	Fixed	SPC/E	12.5(8.6,16.8)	9.8(7.3,12.8)	8.1(4.5,11.7)	0.87(0.68, 0.95)
MBIS	B3LYP/†	OTFP	SPC/E	12.1(8.2,15.5)	8.6(5.8,11.8)	-0.6(-5.2,4.0)	0.87(0.70, 0.96)
MBIS	MP2/†	Fixed	SPC/E	11.4(6.9,16.2)	8.3(5.9,11.4)	7.5(4.3,10.7)	0.88(0.70, 0.97)
MBIS	MP2/†	OTFP	SPC/E	8.7(6.1,11.0)	6.3(4.3,8.5)	-0.8(-4.1,2.5)	0.90(0.75, 0.97)
RESP	B3LYP/†	Fixed	TIP3P	15.5(11.0,20.2)	12.6(9.7,16.1)	11.9(8.1,12.7)	0.81(0.58, 0.92)
RESP	B3LYP/†	OTFP	TIP3P	10.0(6.7,13.3)	7.4(5.2,10.0)	2.2(-1.5,5.9)	0.82(0.58, 0.93)
RESP	HF/6-31G*	Fixed	TIP3P	9.5(6.3,12.5)	6.8(4.6,9.4)	4.4(1.2,7.6)	0.81(0.57, 0.93)
RESP	HF/6-31G*	OTFP	TIP3P	11.5(8.8,14.0)	9.4(7.1,11.9)	-5.8(-9.6,-2.0)	0.83(0.58, 0.94)
AM1–BCC	AM1	Fixed	TIP3P	12.2(7.2,17.6)	8.6(5.9,12.1)	3.2(-1.3,7.7)	0.86(0.69, 0.93)
AM1–BCC	AM1	OTFP	TIP3P	14.0(9.5,18.2)	10.1(6.9,13.8)	-2.9(-8.1,2.3)	0.93(0.83, 0.97)
FreeSolv[12]	AM1	Fixed	TIP3P	10.5(7.3,13.6)	8.2(6.1,10.7)	1.9(-2.0,5.8)	0.93(0.83, 0.97)
Riquelme *et al.*[34] (MBIS)	BLYP/χ	Fixed	SPC/E	11.9(9.3,14.3)	9.8(7.4,12.2)	1.7(-2.8,6.2)	0.83(0.61, 0.94)

deviate positively from experiment (a positive AD value of comparable magnitude to the AAD and an AD confidence interval (CI) that does not contain zero). OTFP reduces the magnitudes of the AD values by over 6.7 kJ·mol^{-1} and results in AD CIs containing zero). The MBIS OTFP results show the smallest AD magnitudes of all charge methods. The Spearman ρ_s is largest for OTFP with MP2, followed by that of B3LYP, then of Riquelme *et al.* however, the CIs of all ρ_s values overlap.

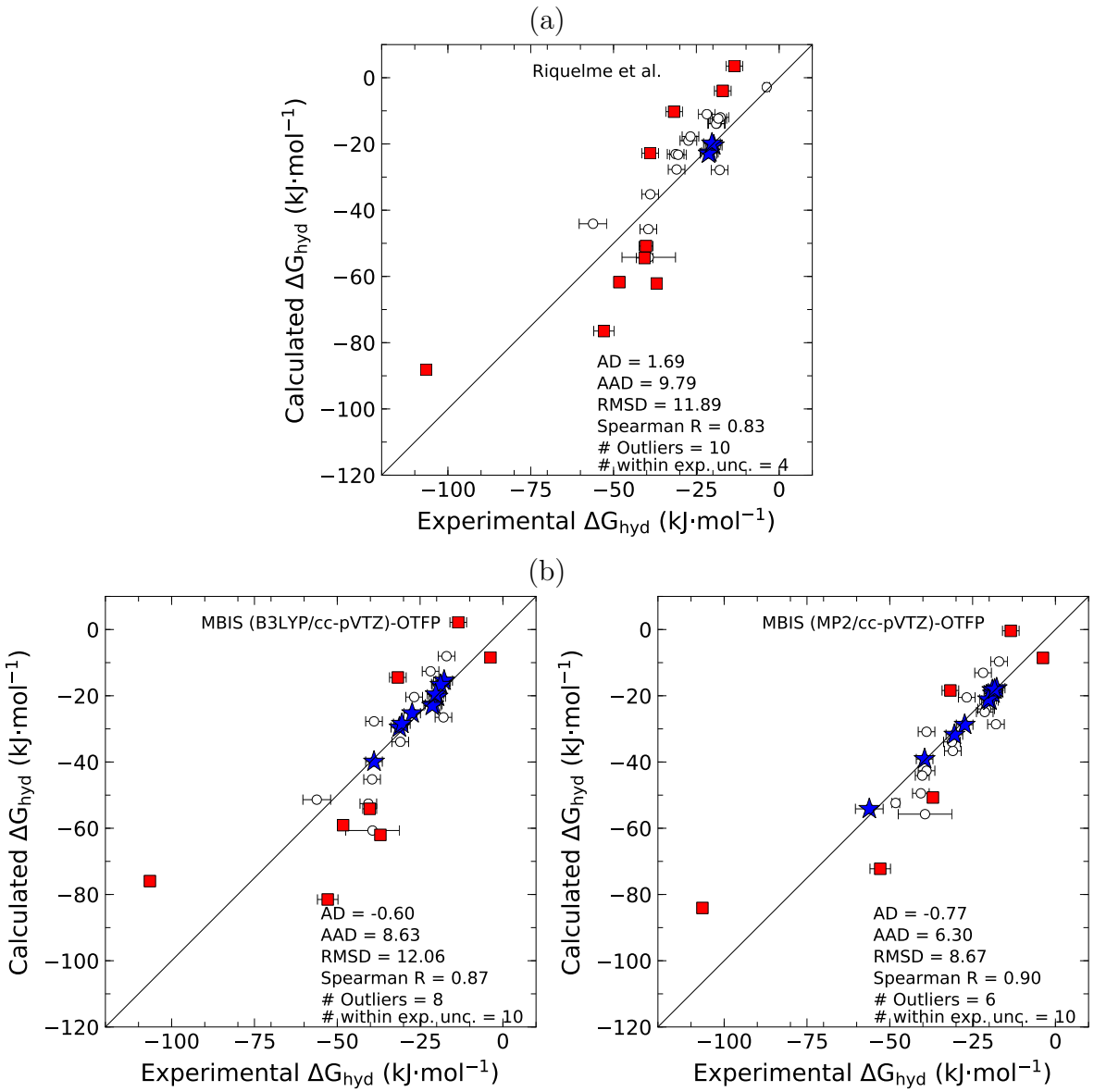

Figure 4: Parity plots comparing calculated and experimental results for ΔG_{hyd} in SPC/E water at $T = 298.15$ K and $P = 1$ bar for the 30 molecules of this study using MBIS–derived partial charges with the SPC/E water model. Fig. (a) shows previous results of Riquelme et al.,[34] Fig. (b) shows our results using the indicated ES theory levels. ★ indicates results whose absolute error e_i satisfies $e_i < \sqrt{\sigma_{expt}^2 + \sigma_{sim}^2}$, where σ_{expt} and σ_{sim} are the respective experimental and simulation uncertainties; ■ indicates Outliers ($e_i > 5\sigma_{expt}$); and ○ indicates results satisfying $\sqrt{\sigma_{expt}^2 + \sigma_{sim}^2} < e_i < 5\sigma_{expt}$. Experimental error bars are shown and simulation error bars are within the symbol sizes.

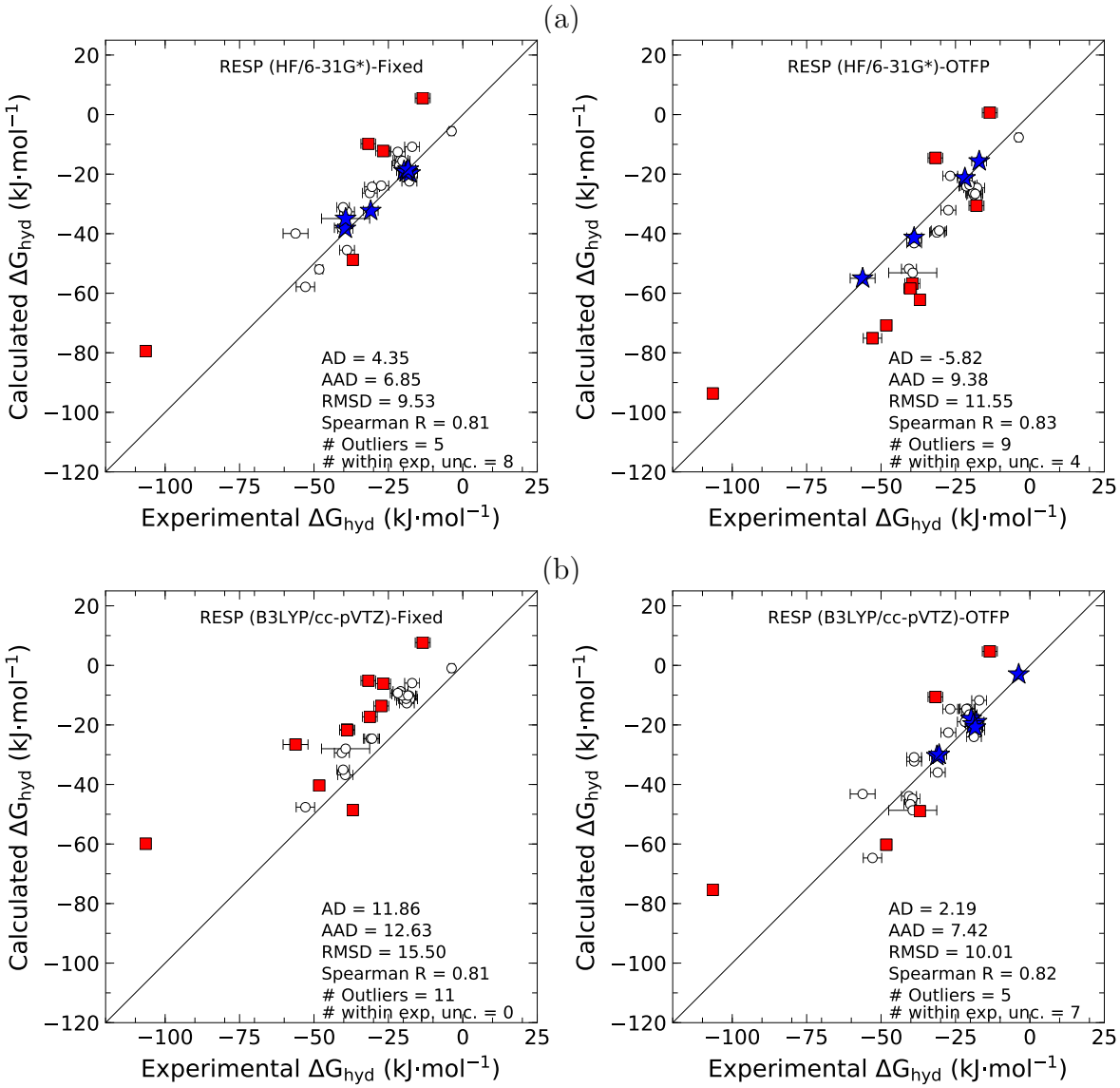

Figure 5: Parity plots comparing experiment and simulated ΔG_{hyd} results using RESP derived partial charges with the TIP3P water model (a): HF/6-31G* fixed charges, upper (b): HF/6-31G* OTFP charges, (c): B3LYP/cc-pVTZ fixed charges, (d): B3LYP/cc-pVTZ OTFP.★ indicates results whose absolute error e_i satisfies $e_i < \sqrt{\sigma_{expt}^2 + \sigma_{sim}^2}$, where σ_{expt} and σ_{sim} are the respective experimental and simulation uncertainties; ■ indicates Outliers ($e_i > 5\sigma_{expt}$); and ○ indicates results satisfying $\sqrt{\sigma_{expt}^2 + \sigma_{sim}^2} < e_i < 5\sigma_{expt}$. Experimental error bars are shown and simulation error bars are within the symbol sizes.

4.2 Hydration free energies using RESP partial charges

Fig. (5) shows parity plots against experimental results using partial charges with TIP3P water, determined by the RESP approach and different levels of theory (5(a) and 5(b)). We

show the corresponding results using the SPC/E water model in the Supporting Information, but we discuss here only the TIP3P results. The figures on the left show results using fixed charges and the figures on the right show results using our OTFP approach. Fig. 5(a) compares results using the GAFF default HF/6-31G* level of theory with those of a higher level of theory and a larger basis set (B3LYP/cc-pVTZ) in Fig. 5(b). We did not expect to see improvements in the AAD when using OTFP with the HF level of theory, since partial charges calculated in the gas phase using HF/6-31G* already contain implicit polarization, so the application of OTFP results in over–polarization.

The Table 2 data indicate that neither fixed–charge nor OTFP results have AD values that contain zero in their confidence interval. This is an example showing that a method, despite having a relatively low AAD, may provide poor predictions. As expected, the use of OTFP with B3LYP/cc-pVTZ improves the corresponding fixed–charged results. While B3LYP with OTFP has a higher AAD than HF/6-31G* fixed–charge it has an AD and confidence interval which includes zero. We conjecture that the B3LYP RESP results can be further improved by using a higher level of theory, as well as a different (larger) basis set, and results can likely be further improved by fitting LJ and torsional parameters to B3LYP/cc-pVTZ derived partial charges.

4.3 Hydration free energies using AM1–BCC

Fig. 6(a) shows parity plots against experimental results for partial charges determined by the AM1–BCC approach. We show corresponding results using the SPC/E water model in the Supporting Information, and note in passing that results are qualitatively the same using the SPC/E or the TIP3P water model. Fig. 6(b) shows AM1–BCC results from the Freesolv database versus experiment, which are discussed in Section 5.3.)

In Fig. 6(a) the left figure shows results using fixed–charges and the right figure shows results using our OTFP approach. The numerical results in Table 2 show that, similarly to the situation for HF/6-31G* partial charges, OTFP leads to over–polarizing the fixed–charge

results, changing the AD from 3.2 kJ·mol^{-1} to -2.9 kJ·mol^{-1}. It also similarly raises the AAD value. The Spearman ρ_s for AM1–BCC shows the largest increase in going from fixed–charge to OTFP (rising from 0.86 to 0.93). Due to the overlapping CIs on the fixed–charge and OTFP ρ_s, the two values cannot be counted as statistically different; however, the CI using OTFP is considerably tighter around the mean value.

5 Discussion

5.1 Dependence on charge method

Since their vacuum phase electron densities do not include significant polarization effects, the most relevant tests of the OTFP method are MBIS using B3LYP and MP2 theories, and RESP using B3LYP, all with the cc-pVTZ basis set (the first six rows of data in Table 2). Their corresponding fixed–charge methodologies expectedly yield poor agreement with experiment, as indicated by the similarity of their AD and AAD values, implying over–prediction. In these cases, the OTFP results consistently yield improvement. This is illustrated in Fig. 5(b) and Figs. S1(a) and S1(b).

In these three cases, the fixed–charge AD 95% CIs do not contain zero, indicating that the hypothesis that each method gives an adequate prediction of the experimental data must be rejected. Conversely, the OTFP CIs all include zero, and the hypothesis cannot be rejected. The OTFP results also have AAD values equal to or smaller than the "gold standard" AM1–BCC fixed–charge result.

The AM1–BCC and HF/6-31G* RESP partial charge sets already implicitly include polarization, and the AD and AAD values of Table 2 indicate a shift from over–prediction of the experimental results to under–prediction with the application of OTFP polarization. This is illustrated in Fig. 5(a). We note that despite fixed–charge RESP HF/6-31G* having one of the lowest AAD values in Table 2, it fails to contain zero in the confidence interval around its AD, which indicates systematic deviations in its predictions for this test set.

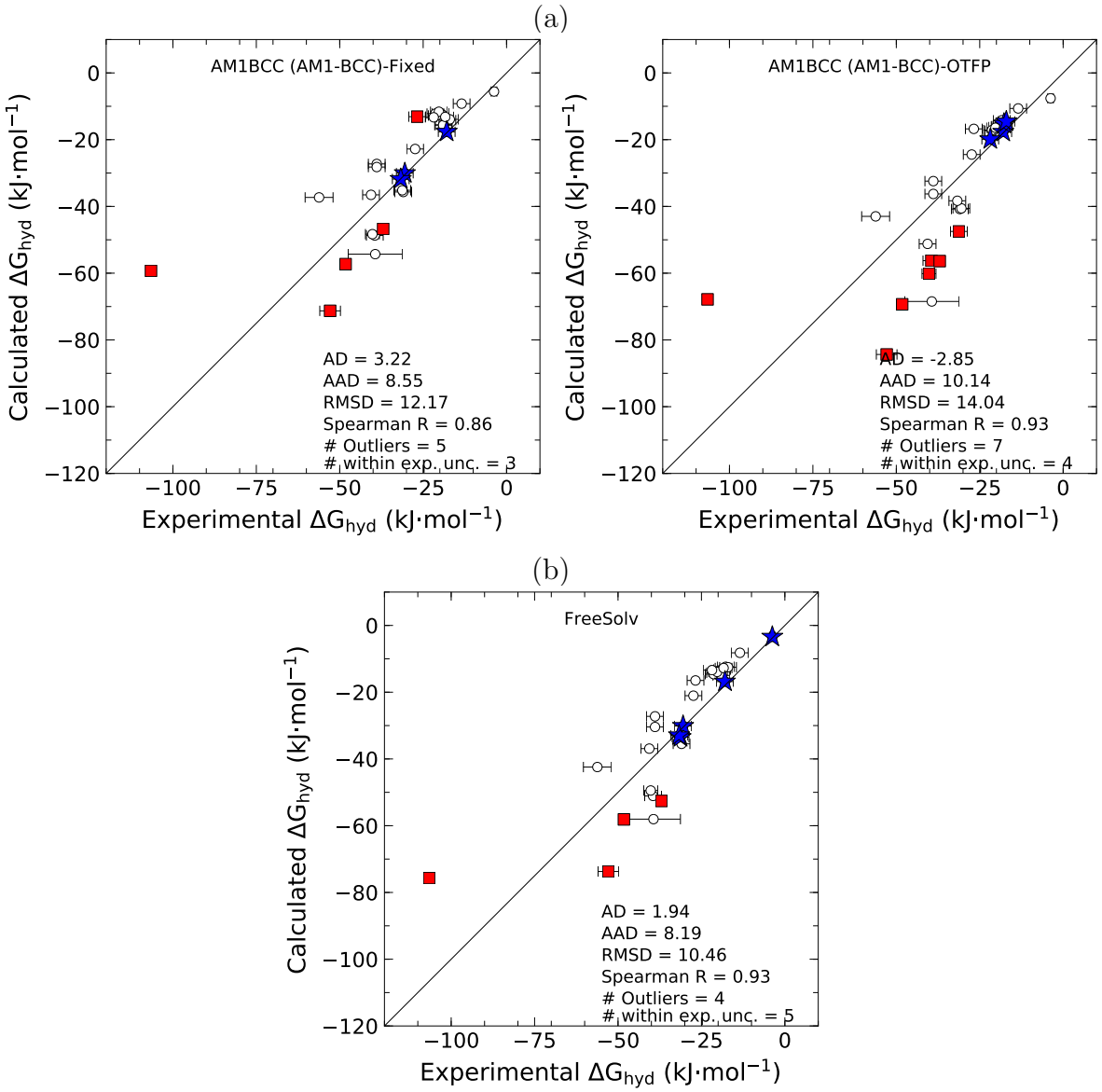

Figure 6: Parity plots comparing experiment and simulated ΔG_{hyd} results using AM1–BCC derived partial charges with the TIP3P water model A: AM1-BCC fixed charges, B: AM1-BCC OTFP, C: FreeSolv database AM1–BCC values.★ indicates results whose absolute error e_i satisfies $e_i < \sqrt{\sigma_{expt}^2 + \sigma_{sim}^2}$, where σ_{expt} and σ_{sim} are the respective experimental and simulation uncertainties ; ■ indicates Outliers ($e_i > 5\sigma_{expt}$); and ○ indicates results satisfying $\sqrt{\sigma_{expt}^2 + \sigma_{sim}^2} < e_i < 5\sigma_{expt}$. Experimental error bars are shown and simulation error bars are within the symbol sizes.

There are many ES theories, basis sets, and partial charge methods that can be used. We have shown, however, that when using RESP or MBIS, the OTFP works well with GAFF, and also that increasing the theory level of the ES calculation leads to improved results.

The structure of the OTFP methodology allows its straightforward implementation for any combination of these ingredients. Its application to the Additive Variational Hirshfeld (AVH) partial charge method developed in a recent thesis,[82] which has been shown to produce "more intuitive" partial charges, than MBIS and other Hirshfeld variants, particularly for nitrogen–containing molecules, seems promising.

5.2 Dependence on molecular structure

Fig. (7) shows a grouping of the AAD results comparing the influences on the ΔG_{hyd} predictions of molecular sizes and shape, and of nitrogen and oxygen. Small molecules and non-cyclic molecules show the lowest AAD across all methods. Oxygen–containing molecules are difficult for all methods; however OTFP using MBIS(MP2), OTFP RESP(B3LYP), and fixed charge RESP (HF/6-31G*) show at least 4 kJ·mol^{-1} smaller AAD than the other methods. The same trend is followed for cyclic molecules. Large molecules are best predicted using OTFP with MBIS(MP2). Our study includes calculations on linear alcohols and alkylamines from C_1–C_4. With the exception of the MP2 predictions of methanol and ethanol, which are 1 kJ·mol^{-1} outside experimental uncertainty, all cases of OTFP using MBIS partial charges perform well, whereas AM1–BCC gives results well outside the indicated experimental uncertainties (generally $\approxeq$ 2.5 kJ·mol^{-1}).

OTFP with MBIS partial charges struggles with the tertiary amine triethylamine, whereas AM1–BCC shows the lowest AAD. (See also our earlier discussion in Section 3 concerning its Coulomb decoupling calculation protocol.) Muddana *et al.*[47] also found that AM1–BCC performed better than IPolQ–Mod for tertiary amines.

Our OTFP approach also exhibits difficulties with both ammonia and benzene, which represent the smallest building blocks for amines and cyclics, respectively. (With the current non–Coulomb FF parameter sets, we found that both could be predicted by MP2 OTFP to within experimental uncertainty by using a double ζ basis (cc-pVDZ) set rather than using the larger triple ζ basis set; however, this might be coincidental.)

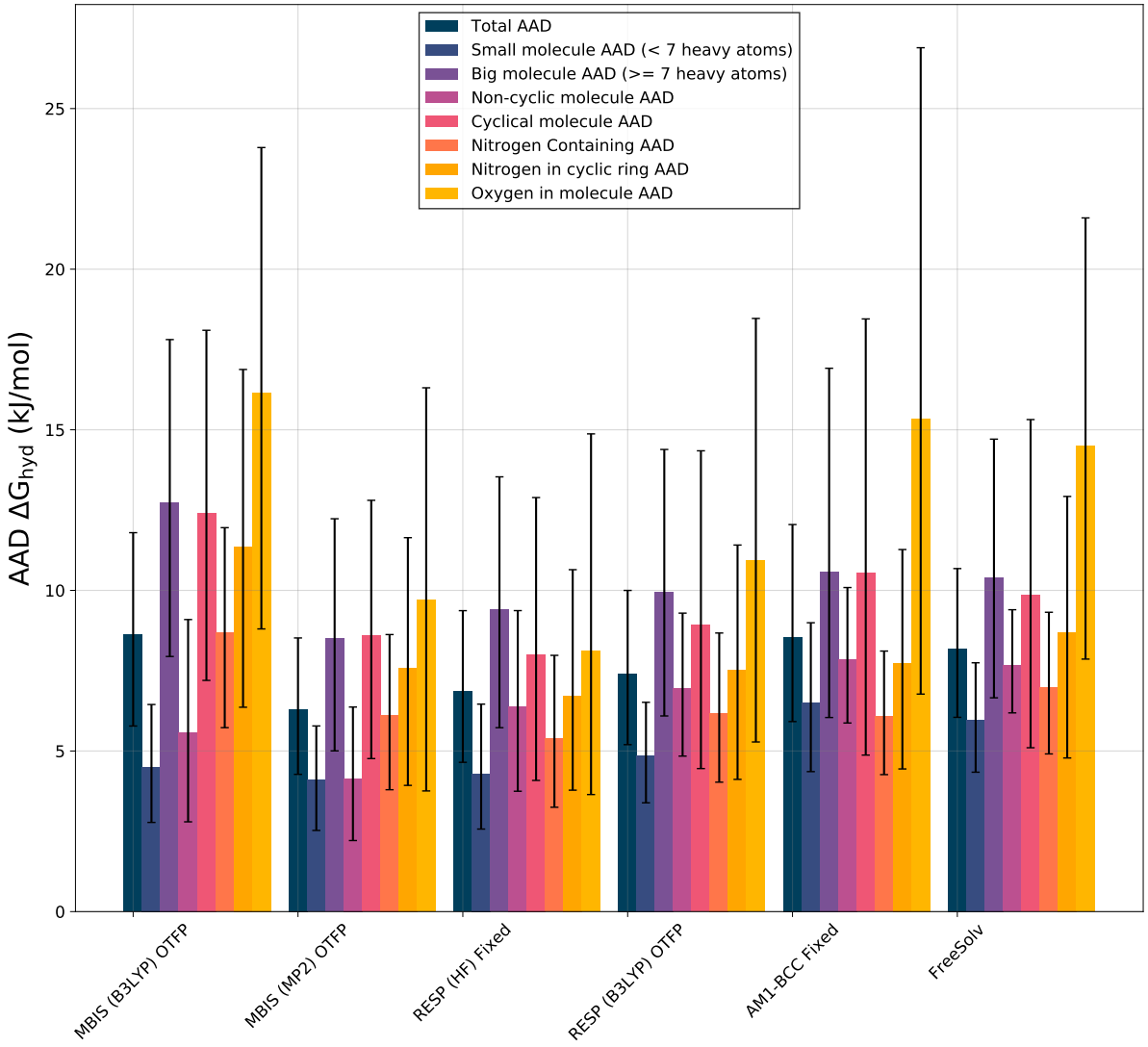

Figure 7: ΔG_{hyd} AAD comparison plot. Error bars indicate 95% uncertainty using the Percentile Bootstrapping method with 100,000 resamples.

Small cyclic molecules are more difficult for all methods, likely because the dipole moment of the ring is unable to leave the plane in an atom–centered charge method. Either out–of–plane charges would be needed, or a charge–on–spring approach, both of which involve additional parameters. In the case of AMOEBA, which already has additional parameters for point dipoles, different polarizability parameters are used for ring–member atoms. It has been noted by Swope *et al.* that for benzene, quadrapole terms contribute more to polarization than dipole terms,[32] and this is possibly also the case for other small cyclic molecules, making

their ΔG_{hyd} predictions especially difficult for standard atom–centered FFs.

We lastly remark that for the 30 molecules common to the MBIS approach of Riquelme *et al.*[34] and present in the FreeSolv database, our MBIS(MP2) results show an AAD of 6.30 kJ·mol^{-1} in comparison with the Riquelme *et al.* AAD value of 9.79 kJ·mol^{-1} and the FreeSolv database values of 8.19 kJ·mol^{-1}. A rough extrapolation to the entire FreeSolv database species would indicate an AAD of around 4.1 kJ·mol^{-1}.

5.3 Potential FF modifications

While the OTFP method only influences the partial charges of the solute molecule, modification of the partial charges has a ripple effect on the accuracy of the remaining FF parameters, most notably the LJ and torsion parameters. GAFF was developed on the basis of fitting LJ and torsion parameters for a particular partial charge set, namely RESP charges calculated from HF/6-31G* electron densities. When the partial charges are not those used in the LJ and torsional optimizations, sub–optimal performance is to be expected by the resulting FF, and the results achieved using OTFP can be expected to improve with refitting of these parameters. A modification to the RESP protocol has recently been proposed which found that predictions of liquid densities and enthalpies of vaporization were improved when the LJ parameters were re–optimized to the new partial charges.[83] In this respect, the very recent method of Kantonen *et al.* for efficiently fitting LJ parameters for MBIS partial charges,[84] should prove to be useful.

An indication of the effects of different LJ and intramolecular FF parameters in the context of the same set of partial charges can be seen by comparing the GAFF(1.7) and GAFF(2.11) AM1–BCC results. This is shown in the parity plot of Fig. (8). The GAFF(1.7) results are those of the FreeSolv database, and the GAFF(2.11) results are our own. Although the two sets of predictions correlate well ($\rho_s = 0.93$), several results differ by nearly 4 kJ·mol^{-1}, and an outlier discussed further below shows a difference of over 16 kJ·mol^{-1}. Table (2) also shows values for RMSD, AAD and AD for both AM1–BCC methods. Despite their identical

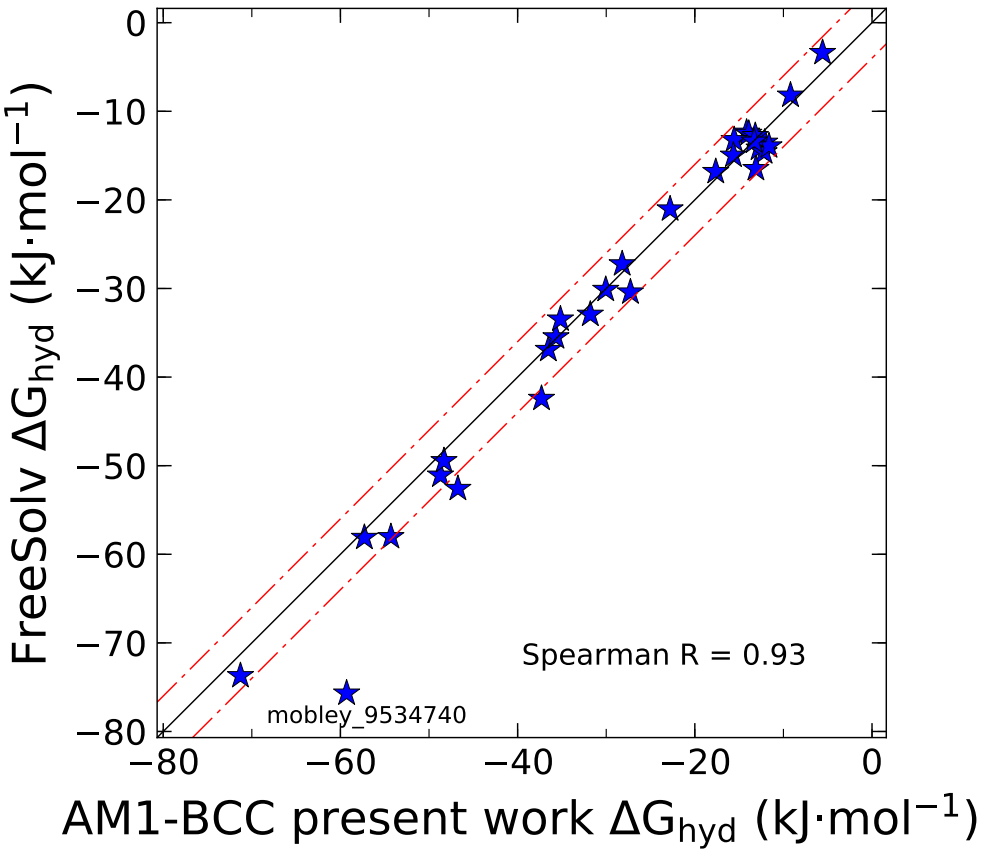

Figure 8: ΔG_{hyd} results for AM1–BCC with GAFF(2.11) compared with FreeSolv, which used AM1–BCC with GAFF(1.7). The red dashed line represents a 4 kJ·mol^{-1} vertical and horizontal deviation from the parity line. mobley_9534740 is (2R, 3R, 4S, 5S,5R)-6-(hydroxymethyl)tetrahydropyran-2,3,4,5-tetrol

partial charges and sharing some (but not all) intramolecular and LJ parameters, GAFF1 has a smaller AAD and an AD that is closer to zero and its CI is better centered around zero than GAFF2.

In this study, three molecules are outliers. Two are included in our results: (2R,3R,4S,5S,6R)–6–(hydroxymethyl)tetrahydropyran–2,3,4,5–tetrol and 2,3–diacetoxypropyl acetate. They are deemed to be outliers because no methods can predict their ΔG_{hyd} values within 5 times their respective experimental uncertainties. A third molecule, 2-hydroxybenzaldehyde is not included in our set of results, since for all the fixed–charge methods the Coulomb window calculations failed to converge, with additional windows exacerbating the failure. This is shown in Figure S4 of the Supporting Information for AM1–BCC partial charges. We

were only able to make the results converge by increasing the magnitudes of the parameters governing the torsional barrier height on the carbonyl group to make the molecule less flexible.

Of the two outliers included in this study, one is a large cyclic and the other a large branched molecule and they both have 6 oxygen atoms. One has 5 hydroxyls and an ether group, while the other has three ester groups. This would seem to indicate that the underlying GAFF parameters for ester and hydroxyl groups perform poorly; however, our results for other molecules containing hydroxyl groups do not indicate serious issues when using OTFP with MBIS. Problems with the ester GAFF parameters have been found by others.[12,34,85] Coupled with the poor results for 2-Hydroxybenzaldehyde, which has a carbonyl oxygen and an alcohol, this seems to indicate that GAFF needs improvement with its carbonyl and ester oxygen parameters.

6 Computational Efficiency

Fig. (9) shows the dependence of ΔG_{hyd} for 2–methoxyethanamine as a function of the number of MD steps between charge updates. For both MBIS and RESP partial charges, 10,000 steps per charge update (used in this study, with the exception of several large molecules noted earlier for which their partial charges were updated every 40,000 steps) is a conservative strategy. Interestingly, MBIS partial charges only need to be updated once every 100,000 MD steps, whereas RESP must be updated once every 40,000 MD steps. This is not surprising, given that RESP is sensitive to molecular geometry and MBIS is much less sensitive.[49]

Fig. (10) shows the ratio of the simulation time required for the OTFP approach with respect to that required for the corresponding fixed–charge approach, as a function of the number of heavy atoms (C/N/O) in the molecule. Fig. 10(a) shows the results using partial charge updates every 10,000 steps and Fig. 10(b) shows the results using partial charge updates every 100,000 steps. As expected, the cost increases with the number of heavy atoms in the molecule. Calculations with MP2 are the most expensive. Both methods using B3LYP

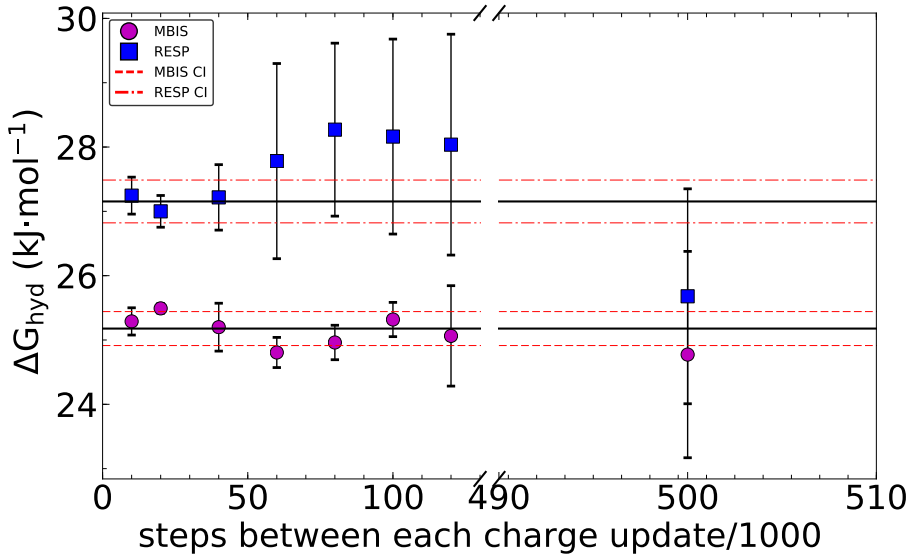

Figure 9: ΔG_{hyd} results for 2-methoxyethanamine as a function of the number of MD steps between charge update intervals. CI in the legend stands for Confidence Interval. Error bars on data are calculated at the Student-t 95% confidence level from 5 independent simulations, and the dashed CI's are calculated using data points up to and including 100,000 steps for MBIS and 40,000 steps for RESP.

(MBIS and RESP) have the same computational cost for the ES electron density calculation, but our implementation of the post–processing step (using a single CPU) to partition the partial charges using MBIS is somewhat more expensive than for RESP.

Fig. 10(b) indicates that for molecules with up to 8 heavy atoms using OTFP with MP2 costs less than a factor of two compared to the cost of a fixed charge simulation, increasing to a factor of roughly an order of magnitude larger for large molecules with 15 or more heavy atoms. When using B3LYP with RESP or MBIS, the OTFP cost reaches roughly twice that of the corresponding fixed–charge for such large molecules.

7 Conclusions

Based on calculations for a diverse test set of 30 neutral molecules, we have demonstrated that fixed charge force–field hydration free energy simulations can be greatly improved by

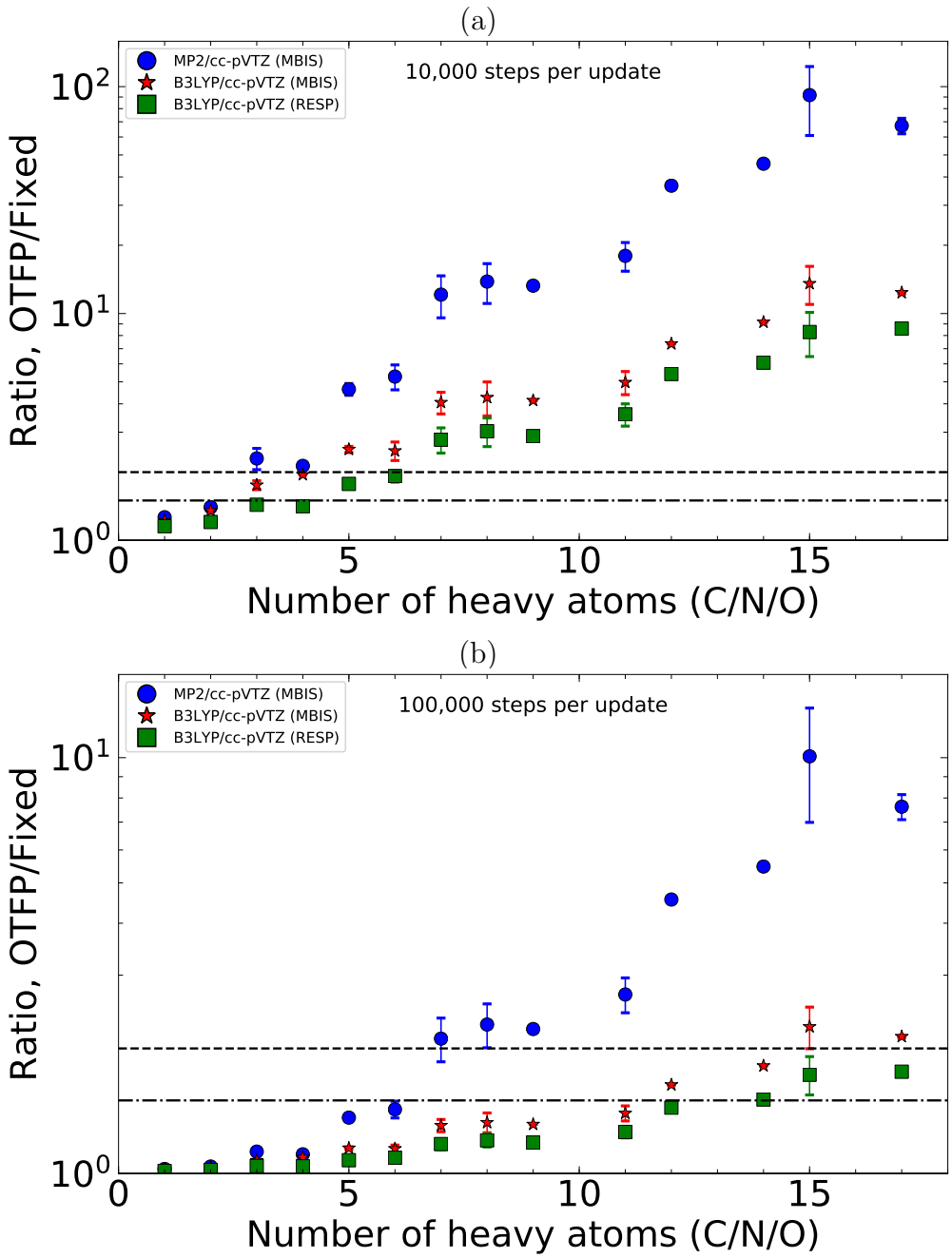

Figure 10: Comparison of computational time required to perform a simulation. (a) OTFP method with partial charge updates occurring every 10,000 steps; (b) OTFP method with 100,000 steps between each partial charge update. The dashed dot line indicates the ratio OTFP/fixed = 1.5. The dashed line indicates the ratio OTFP/fixed = 2.0. Error bars indicate the standard deviation for molecules with the given number of heavy atoms. Each molecule's time is the average of 200 measurements with the exception of the molecules which had their partial charges updated every 40,000 steps, in which case their timing is the average of 50 measurements.

accounting for the solvent's influence on inducing polarity in the solute's partial charges. We have implemented this by updating partial charges on–the–fly and decoupling the solvent electric field appropriately when updating the solute partial charges as its interactions with the solvent are decoupled. By manipulation of double–sided perturbation sampling, we have accounted for the cost of solute self–polarization in a manner similar to that of IPolQ, but with the advantage of maintaining proper polarity, and as a result proper forces and energies, in the endpoint windows. This allows a single ΔG_{hyd} simulation to calculate the free energy difference between an isolated solute with vacuum–derived partial charges and a solute fully polarized when coupled to the solvent.

OTFP using MBIS or RESP partial charges with higher–level theories than HF and basis sets larger than 6-31G* outperforms AM1–BCC in all cases, and in the best case, using MBIS partial charges with electron densities calculated at the MP2/cc-pVTZ level, showed a 2.25 kJ·mol^{-1} lower AAD than that of AM1–BCC. We also showed that RESP using HF/6-31G* systematically deviates from experiment despite having a lower AAD than AM1–BCC. We further showed that the level of QM theory affects the quality of ΔG_{hyd} simulations.

The OTFP method is modular and easy to modify to incorporate different QM theories and basis sets, and different partial charge partitioning schemes can be easily implemented. A convenient feature of this method is that it accounts for polarization without the requirement for any additional parameters beyond those of a classical fixed–charge FF. Although we did not optimize the GAFF parameters to the underlying partial charge method, and we conjecture that optimizing the LJ and torsional parameters with respect to the partial charge method used will further improve the results.

8 Associated Content

The Supporting Information contains the following:

- Raw simulation data for all simulations, parity plots for RESP and AM1–BCC with

SPC/E water models, tables of RMSD and AAD results for all methods and water models used, system size dependence, the equivalence of the Zwanzig and MBAR cost of self–polarization, independent runs vs. MBAR uncertainty estimate comparison, and figures for 2-hydroxybenzaldehyde convergence issues.

- Python code for updating the partial charges (Python code and data files are also available at GitHub:
  https://github.com/BradenDKelly/Alchemical-Free-Energy-OTFP/
- Basic GROMACS files used: *.top, *.gro, *.mdp

The Supporting Information is available free of charge on the ACS Publications website at DOI:xx.xxx/acs.xxx

9 Acknowledgements

The authors acknowledge support provided by the Natural Sciences and Engineering Research Council of Canada (Strategic Program grant no. STPGP 479466-15) and by the SHARCNET (Shared Hierarchical Academic Research Computing Network) HPC Consortium (www.sharcnet.ca) and Compute Canada (www.computecanada.ca). We also express thanks to Professor Paul Ayers for several insightful discussions and to Professor Toon Verstraelen for a plethora of helpful email discussions.

References

(1) Smith, W. R.; Qi, W. Molecular Simulation of Chemical Reaction Equilibrium by Computationally Efficient Free Energy Minimization. *ACS Cent. Sci.* **2018**, *4*, 1185–1193.

(2) Kelly, B.; Smith, W. R. Molecular simulation of chemical reaction equilibria by Kinetic Monte Carlo. *Molecular Physics* **2019**, *117*, 2778–2785.

(3) Noroozi, J.; Smith, W. R. An Efficient Molecular Simulation Methodology for Chemical Reaction Equilibria in Electrolyte Solutions: Application to CO2 Reactive Absorption. *J. Phys. Chem. A* **2018**, *123*, 4074–4086.

(4) Kofke, D. A. Free energy methods in molecular simulation. *Fluid Phase Equilibria* **2005**, *228*, 41–48.

(5) Vega, C.; Sanz, E.; Abascal, J. L. F.; Noya, E. G. Determination of phase diagrams via computer simulation: methodology and applications to water, electrolytes and proteins. *J. Phys. Cond. Matter* **2008**, *20*.

(6) Sanz, E.; Vega, C. Solubility of KF and NaCl in water by molecular simulation. *J.Chem. Phys.* **2007**, *126*.

(7) Moucka, F.; Lisal, M.; skvor, J.; Jirsak, J.; Nezbeda, I.; Smith, W. R. Molecular Simulation of Aqueous Electrolyte Solubility. 2. Osmotic Ensemble Monte Carlo Methodology for Free Energy and Solubility Calculations and Application to NaCl. *J. Phys. Chem. B* **2011**, *115*, 7849–7861.

(8) Mester, Z.; Panagiotopoulos, A. Z. Mean ionic activity coefficients in aqueous NaCl solutions from molecular dynamics simulations. *J.Chem. Phys.* **2015**, *142*, 044507.

(9) Mobley, D. L.; Bayly, C. I.; Cooper, M. D.; Shirts, M. R.; Dill, K. A. Small Molecule Hydration Free Energies in Explicit Solvent: An Extensive Test of Fixed-Charge Atomistic Simulations. *J. Chem. Theory Comput.* **2009**, *5*, 350–358.

(10) Mobley, D. L.; Liu, S.; Cerutti, D. S.; Swope, W. C.; Rice, J. E. Alchemical prediction of hydration free energies for SAMPL. *J. Comput. Aided Mol. Des.* **2012**, *26*, 551–562.

(11) Shivakumar, D.; Williams, J.; Wu, Y.; Damm, W.; Shelley, J.; Sherman, W. Prediction of Absolute Solvation Free Energies using Molecular Dynamics Free Energy Perturbation and the OPLS Force Field. *J. Chem. Theory Comput.* **2010**, *6*, 1509–1519.

(12) Duarte Ramos Matos, G.; Kyu, D. Y.; Loeffler, H. H.; Chodera, J. D.; Shirts, M. R.; Mobley, D. L. Approaches for Calculating Solvation Free Energies and Enthalpies Demonstrated with an Update of the FreeSolv Database. *J. Chem. Eng. Data* **2017**, *62*, 1559–1569.

(13) Gilson, M.; Given, J.; Bush, B.; McCammon, J. The statistical-thermodynamic basis for computation of binding affinities: a critical review. *Biophys. J.* **1997**, *72*, 1047 – 1069.

(14) Grater, F.; Schwarzl, S. M.; Dejaegere, A.; Fischer, S.; Smith, J. C. Protein/Ligand Binding Free Energies Calculated with Quantum Mechanics/Molecular Mechanics. *J. Phys. Chem. B* **2005**, *109*, 10474–10483.

(15) Woo, H.-J.; Roux, B. Calculation of absolute protein–ligand binding free energy from computer simulations. *Proc. Natl. Acad. Sci. U.S.A.* **2005**, *102*, 6825–6830.

(16) Jiao, D.; Golubkov, P. A.; Darden, T. A.; Ren, P. Calculation of protein–ligand binding free energy by using a polarizable potential. *Proc. Natl. Acad. Sci. U.S.A.* **2008**, *105*, 6290–6295.

(17) Deng, Y.; Roux, B. Computations of Standard Binding Free Energies with Molecular Dynamics Simulations. *J. Phys. Chem. B* **2009**, *113*, 2234–2246.

(18) Gill, S. C.; Lim, N. M.; Grinaway, P. B.; Rustenburg, A. S.; Fass, J.; Ross, G. A.; Chodera, J. D.; Mobley, D. L. Binding Modes of Ligands Using Enhanced Sampling (BLUES): Rapid Decorrelation of Ligand Binding Modes via Nonequilibrium Candidate Monte Carlo. *J. Phys. Chem. B* **2018**, *122*, 5579–5598.

(19) Yu, W.; MacKerell, J., Alexander D Computer-Aided Drug Design Methods. *J. Phys. Chem. B* **2017**, *1520*, 85–106.

(20) Cornell, W. D.; Cieplak, P.; Bayly, C. I.; Gould, I. R.; Merz Jr., K. M.; Ferguson, D. M.; Spellmeyer, D. C.; Fox, T.; Caldwell, J. W.; Kollman, P. A. A Second Generation Force Field forthe Simulation of Proteins, Nucleic Acids and Organic Molecules. *J. Am. Chem. Soc.* **1995**, *117*.

(21) Zhou, A.; Schauperl, M.; Nerenberg, P. Benchmarking Electronic Structure Methods for Accurate Fixed-Charge Electrostatic Models. *ChemRxiv* **2019**, *Preprint*.

(22) Fried, S. D.; Wang, L.-P.; Boxer, S. G.; Ren, P.; Pande, V. S. Calculations of the Electric Fields in Liquid Solutions. *J. Phys. Chem. B* **2013**, *117*, 16236–16248.

(23) Rappe, A. K.; Goddard III, W. A. Charge equilibration for molecular-dynamics simulations. *J. Phys. Chem.* **1991**, *95*, 3358–3363.

(24) Rick, S. W.; Stuart, S. J.; Berne, B. Dynamical fluctuating charge force fields: Application to liquid water. *J. Chem. Phys.* **1994**, *101*.

(25) Banks, J. L.; Kaminski, G. A.; Zhou, R.; Mainz, D. T.; Berne, B. J.; Friesner, R. A. Parametrizing a polarizable force field from ab initio data. I. The fluctuating point charge model. *J. Chem. Phys.* **1999**, *110*, 741–754.

(26) Patel, S.; Brooks III, C. L. CHARMM Fluctuating Charge Force Field for Proteins: I Parameterization and Application to Bulk Organic Liquid Simulations. *J. Comput. Chem.* **2003**, *25*, 1–16.

(27) Patel, S.; Mackerell Jr., A. D.; Brooks III, C. L. CHARMM Fluctuating Charge Force Field for Proteins: II Protein/Solvent Properties from Molecular Dynamics Simulations Using a Nonadditive Electrostatic Model. *J. Comput. Chem.* **2004**, *25*, 1504 –1514.

(28) Patel, S.; Brooks III, C. L. Fluctuating charge force fields: recent developments and applications from small molecules to macromolecular biological systems. *Molec. Sim.* **2006**, *32*, 231–249.

(29) Lamoureux, G.; Roux, B. Modeling induced polarization with classical Drude oscillators: Theory and molecular dynamics simulation algorithm. *J. Chem. Phys.* **2003**, *119*, 3025–3039.

(30) Lemkul, J. A.; Huang, J.; Roux, B.; MacKerell Jr, A. D. An Empirical Polarizable Force-Field Based on the Classical Drude Oscillator Model: Development History and Recent Applications‘. *Chem. Rev.* **2016**, *116*, 4983–5013.

(31) Ponder, J. W.; Wu, C.; Ren, P.; Pande, V. S.; Chodera, J. D.; Schnieders, M. J.; Haque, I.; Mobley, D. L.; Lambrecht, D. S.; DiStasio, R. A.; Head-Gordon, M.; Clark, G. N. I.; Johnson, M. E.; Head-Gordon, T. a. Current Status of the AMOEBA Polarizable Force Field. *J. Phys. Chem. B* **2010**, *114*, 2549–2564.

(32) Swope, W. C.; Horn, H. W.; Rice, J. E. Accounting for Polarization Cost When Using Fixed Charge Force Fields. I. Method for Computing Energy. *J. Phys. Chem. B* **2010**, *114*, 8621–8630.

(33) Swope, W. C.; Horn, H. W.; Rice, J. E. Accounting for Polarization Cost When Using Fixed Charge Force Fields. II. Method and Application for Computing Effect of Polarization Cost on Free Energy of Hydration. *J. Phys. Chem. B* **2010**, *114*, 8631–8645.

(34) Riquelme, M.; Lara, A.; Mobley, D. L.; Verstraelen, T.; Matamala, A. R.; Vohringer-Martinez, E. Hydration Free Energies of Organic Molecules in the FreeSolv Database Calculated with Polarized Atom In Molecules Atomic Charges and the GAFF Force Field. *J. Chem. Inf. Model.* **2018**, *58*, 1779–1797.

(35) Jia, X.; Li, P. Solvation Free Energy Calculation Using a Fixed-Charge Model: Implicit

and Explicit Treatments of the Polarization Effect. *J. Phys. Chem. B* **2019**, *123*, 1139–1148.

(36) Giese, T. J.; York, D. M. Development of a Robust Indirect Approach for MM-¿QM Free Energy Calculations That Combines Force–Matched Reference Potential and Bennett's Acceptance Ratio Methods. *J. Chem. Theory Comput.* **0**, *0*, null.

(37) Duarte, F.; Amrein, B. A.; Blaha-Nelson, D.; Kamerlin, S. C. Recent advances in QM/MM free energy calculation using reference potentials. *Biochimica et Biophysica Acta (BBA)* **2015**, *1850*, 954–965.

(38) Ryde, U. How Many Conformations Need To Be Sampled To Obtain Converged QM/MM Energies? The Curse of Exponential Averaging. *J. Chem. Theory Comput.* **2017**, *13*, 5745–5752.

(39) Konig, G.; Brooks, B. R.; Thiel, W.; York, D. M. On the convergence of multi-scale free energy simulations. *Molec. Sim.* **2018**, *44*, 1062–1081.

(40) Woodcock, P. S. H.; Boresch, S.; Rogers, D. M.; Lee, H. Accelerating QM/MM Free Energy Computations via Intramolecular Force Matching. *J. Chem. Theory Comput.* **2018**,

(41) Konig, G.; Pickard, F. C.; Huang, J.; Thiel, W.; MacKerell, A. D.; Brooks, B. R.; York, D. M. A Comparison of QM/MM Simulations with and without the Drude Oscillator Model Based on Hydration Free Energies of Simple Solutes. *Molecules* **2018**, *23*.

(42) Jia, X. Solvation Free Energy Calculations: The Combination between the Implicitly Polarized Fixed-charge Model and the Reference Potential Strategy. *J. Comput. Chem. 0*.

(43) Cerutti, D. S.; Rice, J. R.; Swope, W. C.; Case, D. A. Derivation of Fixed Partial Charges for Amino Acids Accommodating a Specific Water Model and Implicit Polarization. *J. Phys. Chem. B* **2013**, *117*, 2328–2338.

(44) Bayly, C. I.; Cieplak, P.; Cornell, D., Wendy; Kollman, P. A. A Well-Behaved Electrostatic Potential Based Method Using Charge Restraints for Deriving Atomic Charges: The RESP Model. *J. Phys. Chem.* **1993**, *97*, 10269–10280.

(45) Cerutti, D. S.; Swope, W.; Rice, J. E.; Case, D. A. ff14ipq: A Self-Consistent Force Field for Condensed-Phase Simulations of Proteins. *J. Chem. Theory Comput.* **2014**, *10*, 4515–4534.

(46) Debiec, K. T.; Cerutti, D. S.; Baker, L. R.; Gronenborn, A. M.; Case, D. A.; Chong, L. T. Further Along the Road Less Travelled: AMBER ff15ipq, an Original Protein Force Field Built on a Self-Consistent Physical Model. *J. Chem. Theory Comput.* **2016**, *12*, 3926–3947.

(47) Muddana, H.; Sapra, N.; Fenley, A.; Gilson, M. The SAMPL4 hydration challenge: evaluation of partial charge sets with explicit-water molecular dynamics simulations. *J. Comput. Aided Mol. Des.* **2014**, *28*, 277–287.

(48) Mecklenfeld, A.; Raabe, G. Comparison of RESP and IPolQ-Mod Partial Charges for Solvation Free Energy Calculations of Various Solute/Solvent Pairs. *J. Chem. Theory Comput.* **2017**, *13*, 6266–6274.

(49) Verstraelen, T.; Vandenbrande, S.; Heidar-Zadeh, F.; Vanduyfhuys, L.; Van Speybroeck, V.; Waroquier, M.; Ayers, P. W. Minimal Basis Iterative Stockholder: Atoms in Molecules for Force-Field Development. *J. Chem. Theory Comput.* **2016**, *12*, 3894–3912.

(50) Wang, J.; Wolf, R. M.; Caldwell, J. W.; Kollman, P. A.; Case, D. A. Development and testing of a general AMBER force field. *J. Comput. Chem.* **2004**, *25*, 1157–1174.

(51) Jakalian, A.; Bush, B. L.; Jack, D. B.; Bayly, C. I. Fast, Efficient Generation of High-Quality Atomic Charges. AM1-BCC Model: I. Method. *J. Phys. Chem.* **2000**, *21*, 132–146.

(52) Marenich, A. V.; Cramer, C. J.; Truhlar, D. G. Universal Solvation Model Based on Solute Electron Density and on a Continuum Model of the Solvent Defined by the Bulk Dielectric Constant and Atomic Surface Tensions. *J. Chem. Phys. B* **2009**, *113*, 6378–6396.

(53) Reddy, M. R.; Singh, U.; Erion, M. D. Ab Initio Quantum Mechanics-Based Free Energy Perturbation Method for Calculating Relative Solvation Free Energies. *J. Comput. Chem.* **2006**, *28*, 491–494.

(54) Reddy, M. R.; Singh, U. C.; Erion, M. D. Use of a QM/MM-Based FEP Method to Evaluate the Anomalous Hydration Behavior of Simple Alkyl Amines and Amides: Application to the Design of FBPase Inhibitors for the Treatment of Type-2 Diabetes. *J. Am. Chem. Soc.* **2011**, *133*, 8059–8061.

(55) Rathmore, R.; Sumakanth, M.; Reddy, M.; Reddanna, P.; Rao, A. A.; Erion, M. D.; Reddy, M. Advances in Binding Free Energies Calculations: QM/MM–Based Free Energy Perturbation Method for Drug Design. *Curr. Pharm. Des.* **2013**, *19*, 4674–4686.

(56) Rosta, E.; Haranczyk, M.; Chu, Z. T.; Warshel, A. Accelerating QM/MM Free Energy Calculations: Representing the Surroundings by an Updated Mean Charge Distribution. *J. Phys. Chem. B* **2008**, *112*, 5680–5692.

(57) Maranon, J.; Grigera, J. Molecular Dynamics simulation with partial charges update of erythtrol in water. *Theochem* **1998**, *431*, 7–15.

(58) Maranon, J.; Grigera, J. Variable charge molecular dynamics simulation—adenine molecule in water. *J. Mol. Struct.* **1999**, *490*, 243–248.

(59) Roy Kimura, S.; Rajamani, R.; Langley, D. R. Communication: Quantum polarized fluctuating charge model: A practical method to include ligand polarizability in biomolecular simulations. *J. Chem. Phys.* **2011**, *135*.

(60) Pronk, S.; Pall, S.; Schulz, P. B. P., R.; Larsson; Apostolov, M., R. ad Shirts; Smith, J.; Kasson, P.; van der Spoel, B., D.and Hess; Lindahl, E. GROMACS 4.5: a high-throughput and highly parallel open source molecular simulation toolkit. *Bioinformatics* **2013**, *2019*.

(61) Deppmeier, B.; Driessen, A.; Hehre, W. J.; Johnson, J. A.; Ohlinger, S.; Klunzinger, P. E. Spartan'18. Wavefunction Inc., Irvine, CA.

(62) Wang, J.; Wang, W.; A., K. P.; Case, D. A. Automatic atom type and bond type perception in molecular mechanical calculations. *J. Mol. Graph. Model.* **2006**, *25*.

(63) Verstraelen, T.; Tecmer, P.; Heidar-Zadeh, F.; Boguslawski, K.; Chan, M.; Zhao, Y.; Kim, T. D.; Vandenbrande, S.; Yang, D.; González-Espinoza, C. E.; Fias, S.; Limacher, P. A.; Berrocal, D.; Malek, A.; Ayers, P. W. Helpful Open-source Research TOol for N-fermion systems HORTON 2.0.0. **2015**,

(64) Frisch, M. J. et al. Gaussian˜16 Revision C.01. 2016; Gaussian Inc. Wallingford CT.

(65) Sousa da Silva, A. W.; Vranken, W. F. ACPYPE - AnteChamber PYthon Parser interfacE. *BMC Research Notes* **2012**, *5*.

(66) Senthilkumar, K.; Mujika, J. I.; Ranaghan, K. E.; Manby, F. R.; Mulholland*, A. J.; Harvey, J. N. Analysis of polarization in QM/MM modelling of biologically relevant hydrogen bonds. *J. Roy Soc. Interface* **2008**, *5*.

(67) Hickey, A. L.; Rowley, C. N. Benchmarking Quantum Chemical Methods for the Calculation of Molecular Dipole Moments and Polarizabilities. *J. Phys. Chem. A* **2014**, *118*.

(68) ROCS, OpenEye Scientific Software, Santa Fe,http://www.eyesopen.com.

(69) Cramer, C. J. *Essentials of Computational Chemistry: Theories and Models*, 2nd ed.; John Wiley & Sons: West Sussex, 2004.

(70) Karamertzanis, P.; Raiteri, P.; Galindo, A. The use of anisotropic potentials in modeling water and free energies of hydration. *J. Chem. Theory Comput.* **2010**, *6*, 1590–1607.

(71) Berendsen, H.; Grigera, J. R.; Straatsma, T. P. The missing Term in Effective Pair Potentials. *J. Phys. Chem.* **1987**, *91*, 6269–6271.

(72) Jorgensen, W. L.; Chandrasekhar, J.; Madura, J. D.; Impey, R. W.; Klein, M. Comparison of Simple Potential Functions for Simulating Liquid Water. *J. Chem. Phys.* **1983**, *79*, 926–935.

(73) Abraham, M.; van der Spoel, D.; E. Lindahl, B. H.; the GROMACS development team, 2017; GROMACS User Manual version 2016.3, www.gromacs.org.

(74) Bondi, A. van der Waals Volumes and Radii. *J. Phys.Chem.* **1964**, *68*.

(75) Van Gunsteren, W. F.; Berendsen, H. J. C. A Leap-frog Algorithm for Stochastic Dynamics. *Molec. Sim.* **1988**, *1*, 173–185.

(76) Shirts, M. R.; Chodera, J. D. Statistically optimal analysis of samples from multiple equilibrium states. *J. Chem. Phys.* **2008**, *129*, 124105.

(77) Klimovich, P.; Shirts, M.; Mobley, D. Guidelines for the analysis of free energy calculations. *J Comput Aided Mol Des* **2015**, *29*, 397–411.

(78) Aggarwal, R.; Ranganathan, P. Common pitfalls in statistical analysis: The use of correlation techniques. *Perspect Clin Res* **2016**, *7*, 187–190.

(79) Ranganathan, P.; Pramesh, C. S.; Aggarwal, R. Common pitfalls in statistical analysis: Measures of agreement. *Perspect Clin Res* **2017**, *8*, 187–191.

(80) *Handbook of Applicable Mathematics*; Wiley–Interscience, 1984; Vol. VI.

(81) Chernick, M. R. *Bootstrap Methods: A Guide for Practitioners and Researchers*; Wiley–Interscience: Hoboken, NJ, 2008.

(82) Heidar Zadeh, F. Variational Information-Theoretic Atoms-in-Molecules. Ph.D. thesis, McMaster University & University of Ghent, 2017.

(83) Schauperl, M.; Nerenberg, P.; Jang, H.; Wang, L.-P.; Bayly, C. I.; Mobley, D.; Gilson, M. Force Field Partial Charges with Restrained Electrostatic Potential 2 (RESP2). *chemRxiv* **2019**,

(84) Kantonen, S.; Muddana, H. S.; Henriksen, N. M.; Wang, L.-P.; Gilson, M. Optimized Mapping of Gas-Phase Quantum Calculations to General Force Field Lennard-Jones Parameters Based on Liquid-State Data. *chemRxiv* **2019**,

(85) Fennell, C. J.; Wymer, K. L.; Mobley, D. L. A Fixed-Charge Model for Alcohol Polarization in the Condensed Phase, and Its Role in Small Molecule Hydration. *J. Chem. Phys B* **2014**, *118*, 6438–6446.